ORDER OF PRESENTATION

- SOLID PROPELLANT REGRESSION RATE MEASUREMENT
  - MICROWAVE DOPPLER SHIFT TECHNIQUE
    (FOR MEASUREMENT OF PROPELLANT COMBUSTION RESPONSE FUNCTION)
  - PLASMA CAPACITANCE GAGE TECHNIQUE
    (FOR MEASUREMENT OF EROSIVE AUGMENTATION OF PROPELLANT BURNING RATE)
- HYBRID ROCKET COMBUSTION INSTABILITY MECHANISMS
- MINIATURIZED COMPONENTS FOR FUTURE SPACECRAFT PROPULSION SYSTEMS

MICROWAVE DOPPLER SHIFT PROPELLANT BURNING RATE MEASUREMENT TECHNIQUE

JPL

ROCKET MOTOR STABILITY PREDICTION

- ROCKET CHAMBER PRESSURE DISTURBANCE VARYING SINUSOIDALLY IN TIME

$$P' = \hat{P} e^{i\omega t} e^{\alpha t}$$

- EXPONENTIAL COEFFICIENT α HAS GENERAL FORM

$$\alpha = R_{PC}^{(r)} I_{PC} + R_{VC}^{(i)} I_{VC} + \alpha_{FT} + \alpha_{PD} + R_N^{(r)} I_N + \alpha_{ST}$$

WHERE: $R_{PC} = \dfrac{m_b' / \bar{m}_b}{P' / \bar{P}}$ $\quad R_{VC} = \dfrac{m_b' / \bar{m}_b}{v' / \bar{a}}$

Definition of solid propellant pressure-coupled combustion response function

R_N	=	NOZZLE RESPONSE FUNCTION
I	=	ACOUSTIC STABILITY INTEGRALS
α_{FT}	=	FLOW TURNING COEFFICIENT
α_{PD}	=	PARTICLE DAMPING COEFFICIENT
α_{ST}	=	STRUCTURAL DAMPING COEFFICIENT

JPL

ACOUSTIC ADMITTANCE

ACOUSTIC ADMITTANCE OF PROPELLANT BURNING SURFACE

$$A_{PC} = \frac{u'/\bar{a}}{P'/\gamma\bar{P}} \qquad A_{VC} = \frac{u'/\bar{a}}{v'/\bar{a}}$$

RESPONSE FUNCTION AND ACOUSTIC ADMITTANCE RELATED BY BURNING SURFACE MASS BALANCE

$$A_b + \bar{M}_b = \gamma \bar{M}_b R_b$$

$\bar{M}_b$ = mean Mach No. of propellant surface gas evolution.

Relationship between combustion response function and acoustic admittance

DESCRIPTION OF

MICROWAVE BURNING RATE MEASUREMENT TECHNIQUE

J. of Spacecraft and Rockets, Vol. 17, No. 6

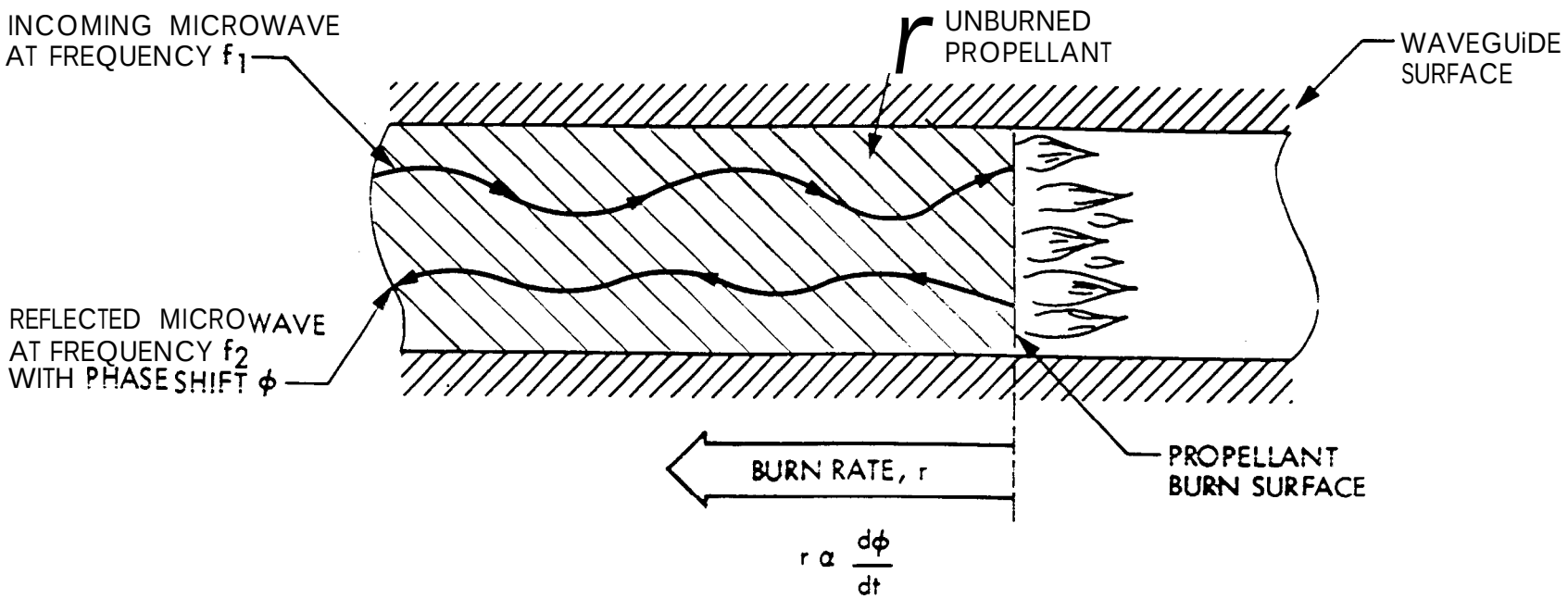

Rate of regression of propellant surface proportional to time rate of change of the Doppler phase shift.

J. of Spacecraft and Rockets, Vol. 17, No. 6

Microwave Doppler shift technique for measuring solid propellant combustion response to oscillatory pressure

EXPERIMENTAL TECHNIQUE

COMBUSTION RESPONSE FUNCTION

$$R_b \equiv \frac{m'/\bar{m}}{P'/\bar{P}} = \frac{\rho r'/\rho\bar{r}}{P'/\bar{P}} = \frac{r'/\bar{r}}{P'/\bar{P}} \tag{1}$$

MICROWAVE DOPPLER SHIFT MEASUREMENT

$$r = \frac{1}{2k_p}\frac{d\phi}{dt} \tag{2}$$

FROM EQN. (2):

$$\bar{r} = \frac{1}{2k_p}\dot{\bar{\phi}} \tag{3}$$

AND FOR A SINUSOIDALLY VARYING P', ($P' = \Delta P e^{i\omega t}$):

$$\phi' = \Delta\phi e^{i(\omega t + \theta)} \tag{4}$$

Phase angle between ϕ' and P'

AND $r' = \frac{d\phi'}{dt}\Big/2k_p$

$$= i\omega\Delta\phi e^{i(\omega t + \theta)}/2k_p$$

$$= 2\pi f\Delta\phi e^{i(2\pi f + \theta + \pi/2)}/2k_p \tag{5}$$

EXPERIMENTAL TECHNIQUE (Cont'd)

COMBINING $\bar{r}$ AND r' RESULTS WITH MEASURED PRESSURE INFORMATION ($\bar{P}$, P'), FROM EQN. (1):

$$R_b = \frac{r'/\bar{r}}{P'/\bar{P}}$$

$$= \frac{2\pi f \Delta\phi}{\dot{\bar{\phi}}} \frac{\bar{P}}{\Delta P} e^{i(\theta + \pi/2)} \qquad (6)$$

SETTING $\dot{\bar{\phi}} = 360°/\Delta t$, WHERE At IS THE PERIOD FOR A 360° SHIFT IN PHASE:

$$R_b = \frac{2\pi f \Delta\phi \Delta t}{360°} \frac{\bar{P}}{\Delta P} e^{i(\theta + \pi/2)} \qquad (7)$$

$$= |R_b| e^{i(\theta + \pi/2)}$$

CALCULATED MINIMUM MEASURABLE ABSOLUTE VALUE OF RESPONSE FUNCTION vs. FREQUENCY

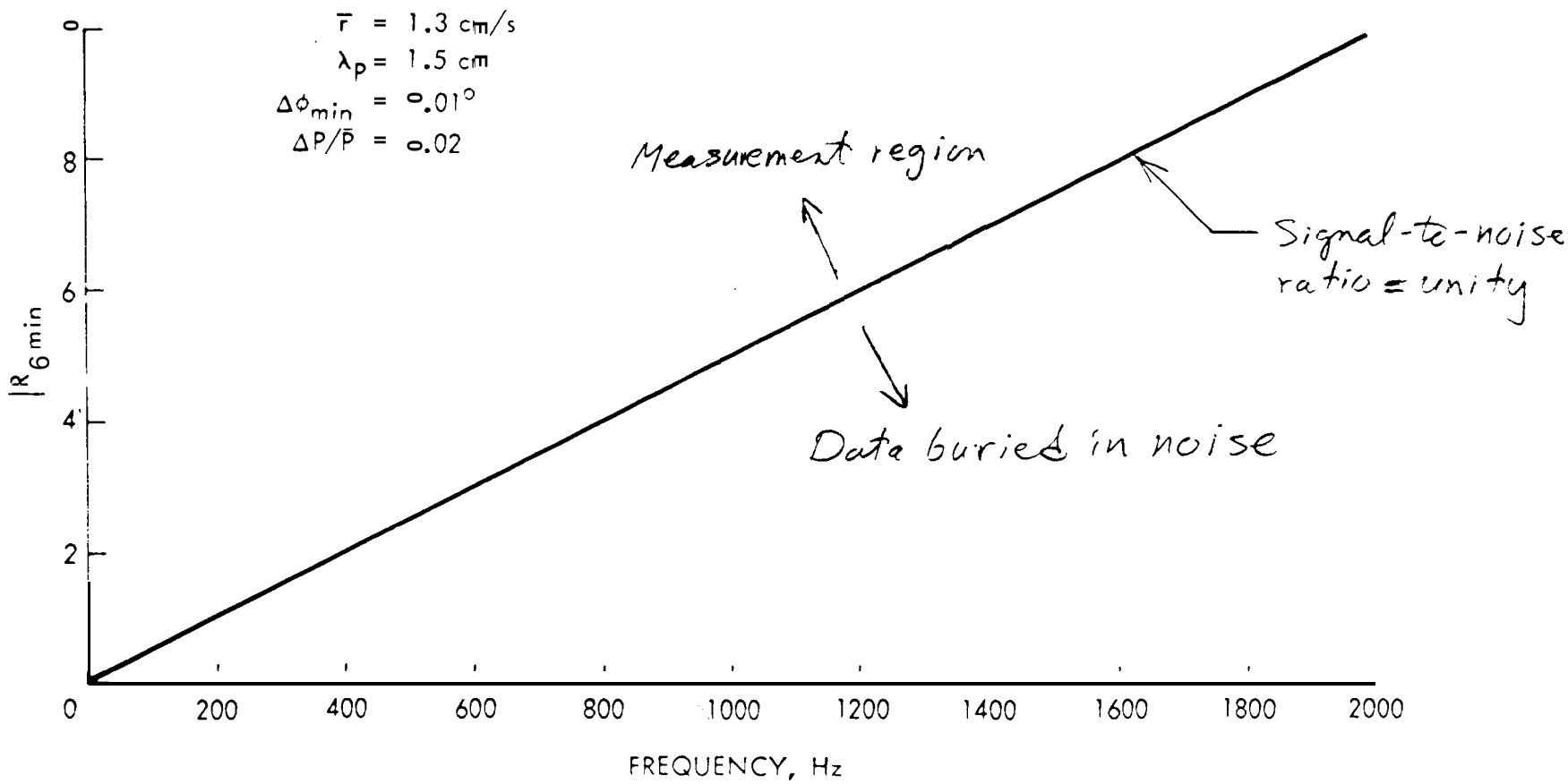

Minimum measurable response function limited by oscillatory phase measurement resolution, $\Delta\phi_{min}$, (which is fixed) and pressure modulation amplitude, $\Delta P/\bar{P}$.

DESCRIPTION OF JPL RESEARCH TO MEASURE

JPL COMBUSTION RESPONSE TO OSCILLATORY RADIANT HEAT FLUX

- OBJECTIVE:
  - UPPER FREQUENCY LIMIT OF MICROWAVE DOPPLER VELOCIMETER TECHNIQUE FOR MEASURING PRESSURE-COUPLED RESPONSE FUNCTION (R_p) OF SOLID PROPELLANTS IS ~1 KHz, LIMITED PRIMARILY BY LIMITING AMPLITUDE OF DRIVEN PRESSURE OSCILLATIONS IN MICROWAVE BURNER. OBJECTIVE IS TO DEVELOP REVISED SYSTEM CAPABLE OF MAKING MEASUREMENTS AT FREQUENCIES UP TO 2 KHz AND MORE

- APPROACH:
  - USE MICROWAVE DOPPLER VELOCIMETER TO MEASURE COMBUSTION RESPONSE TO OSCILLATING THERMAL RADIATION SOURCE (LASER) RATHER THAN PRESSURE. RELATE MEASURED BURNING RATE RESPONSE TO THERMAL RADIATION (R_q) TO EQUIVALENT OSCILLATION IN PRESSURE USING EXISTING THERMAL COMBUSTION THEORY

$$R_p = R_q \left[\frac{q'/q_o}{p'/p_o} \right]$$

Theoretical transfer function between oscillatory pressure and propellant heating flux

AIAA 89-2667

DEFINITION OF

OSCILLATORY HEAT FLUX RESPONSE FUNCTION

JPL

$$R_q = \frac{r'/\bar{r}}{q'/\bar{q}} = \frac{r'}{q'} \Big/ \frac{\bar{r}}{\bar{q}}$$

$$r' = f(d\phi'/dt)$$
$$\bar{r} = f(d\bar{\phi}/dt) = f(\dot{\bar{\phi}})$$

FOR A SINUSOIDALLY VARYING q'

Phase angle between ϕ' and q'

$$R_q = \left[\frac{\omega \Delta \phi}{\Delta q} \Big/ \frac{\dot{\bar{\phi}}}{\bar{q}} \right] e^{i(\theta + \pi/2)}$$

$$= \left[\frac{2\pi f \Delta\phi_{mean}}{\Delta q_{mean}} \Big/ \frac{\dot{\bar{\phi}}_{CW} - \dot{\bar{\phi}}_0}{\Delta q_{CW}} \right] e^{i(\theta + \pi/2)}$$

Argument of response

Absolute value of response

Continuous wave

AIAA 87-0562 Theoretical pressure coupled response function model

JPL

CALCULATED TRANSFER FUNCTION vs FREQUENCY FOR TYPICAL AP COMPOSITE PROPELLANT

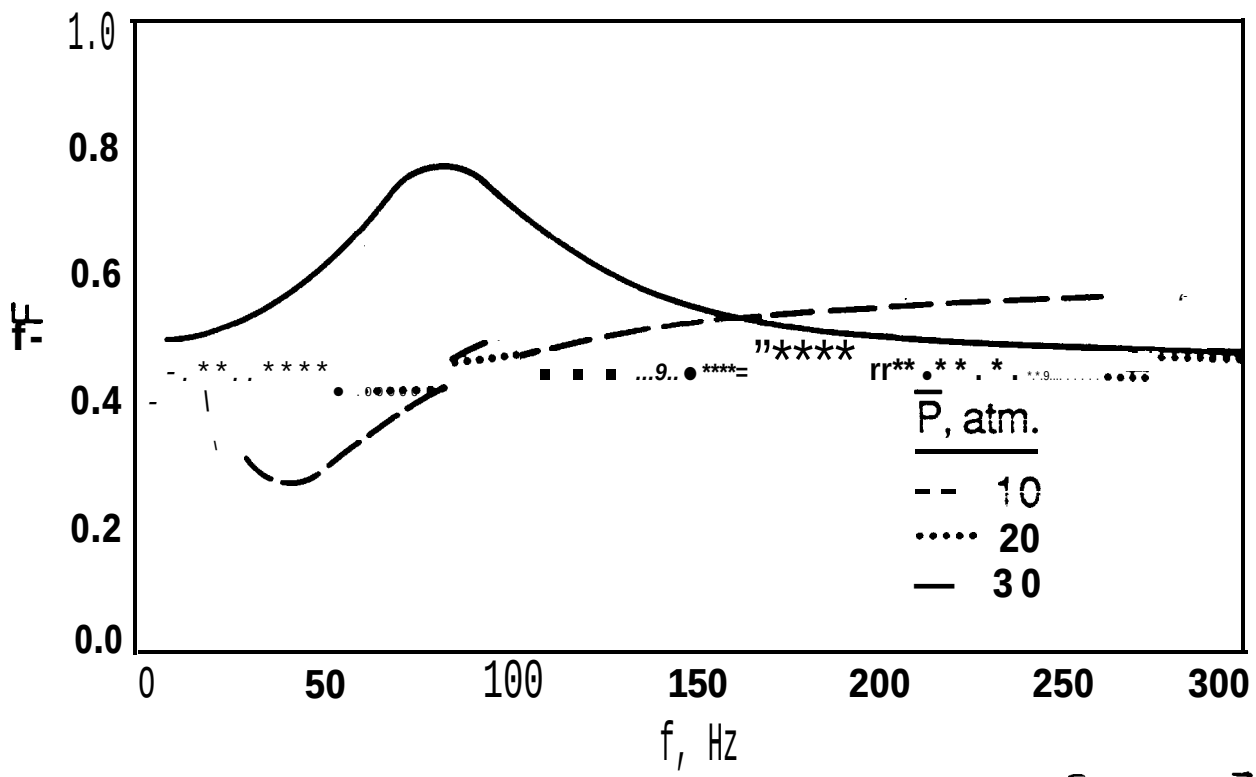

$$TF = \left[\frac{q'/\bar{q}}{p'/\bar{p}}\right]$$

AIAA 89-2667

JPL A SECOND TRANSFER FUNCTION ANALYSIS

$$\frac{q'/\bar{q}}{p'/\bar{p}} = \frac{dq/\bar{q}}{dp/\bar{p}}$$

THERMAL ANALYSIS OF SOLID PHASE YIELDED

$$\frac{dq/\bar{q}}{dp/\bar{p}} = n$$, the propellant burning rate pressure exponent

AIAA 89-2667

JPL

SCHEMATIC OF TEST CONCEPT

using microwave Doppler velocimeter technique to measure the propellant combustion response to an incident, oscillating thermal radiation source (CO_2 laser).

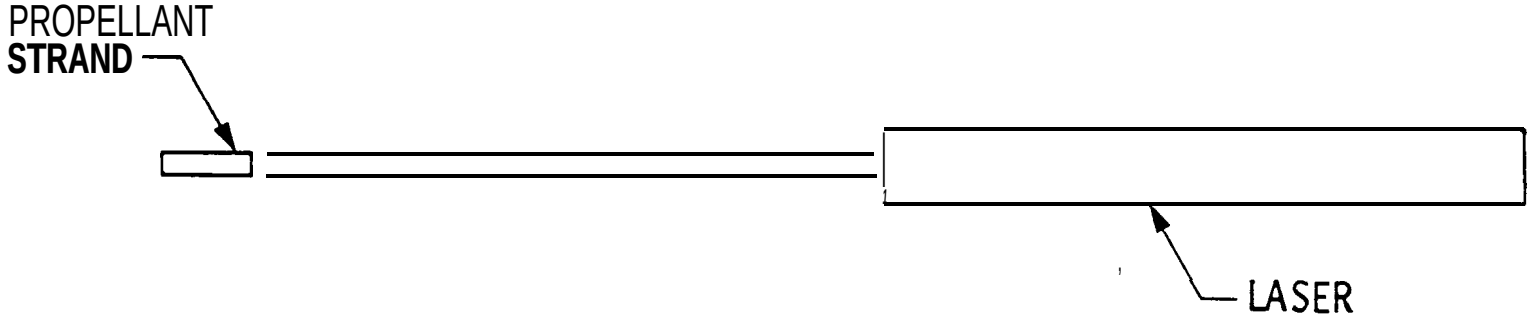

AIAA 89-2667

JPL

SCHEMATIC OF MICROWAVE SYSTEM

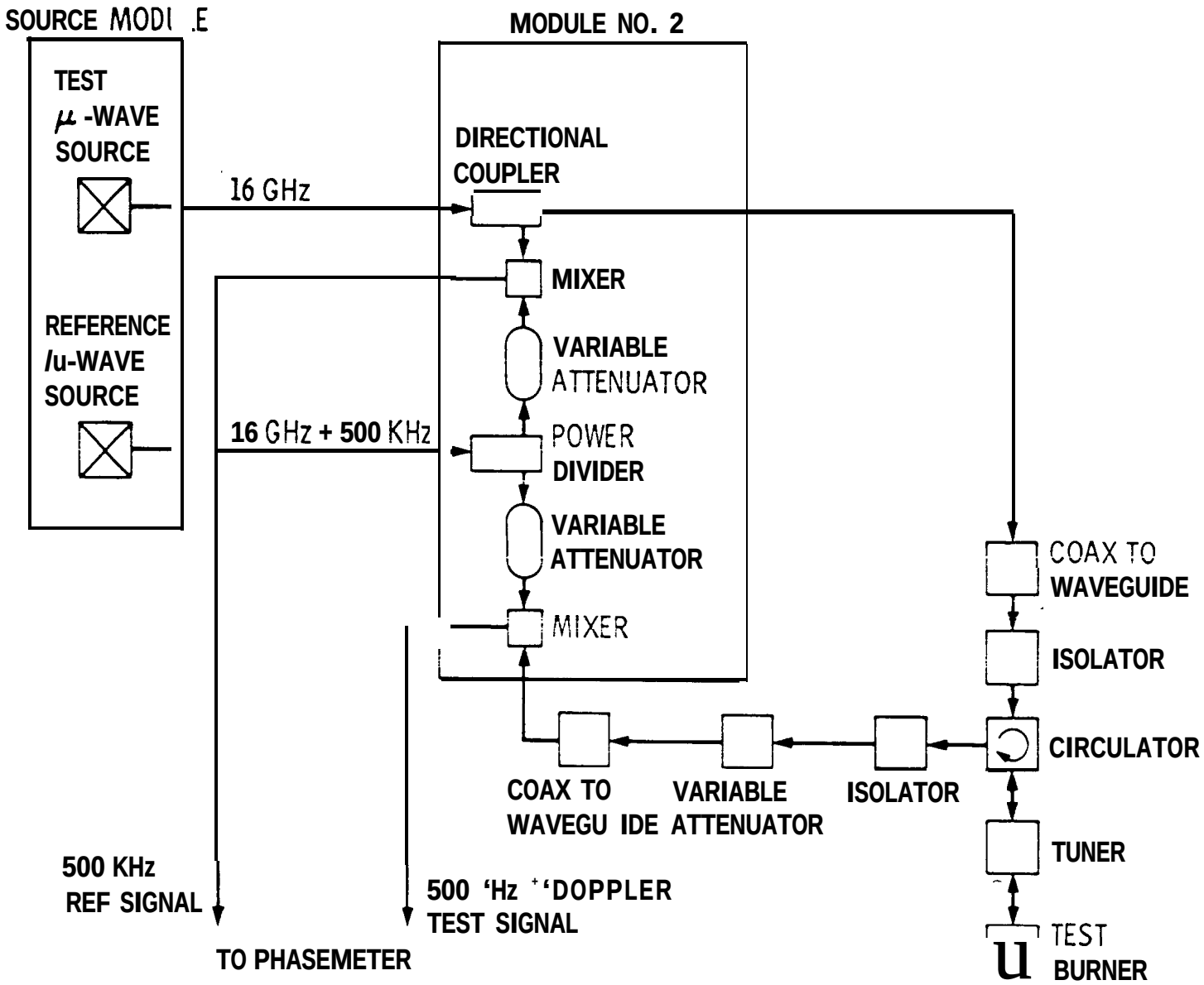

AIAA 89-2667

JPL MICROWAVE WINDOW BURNER ASSEMBLY

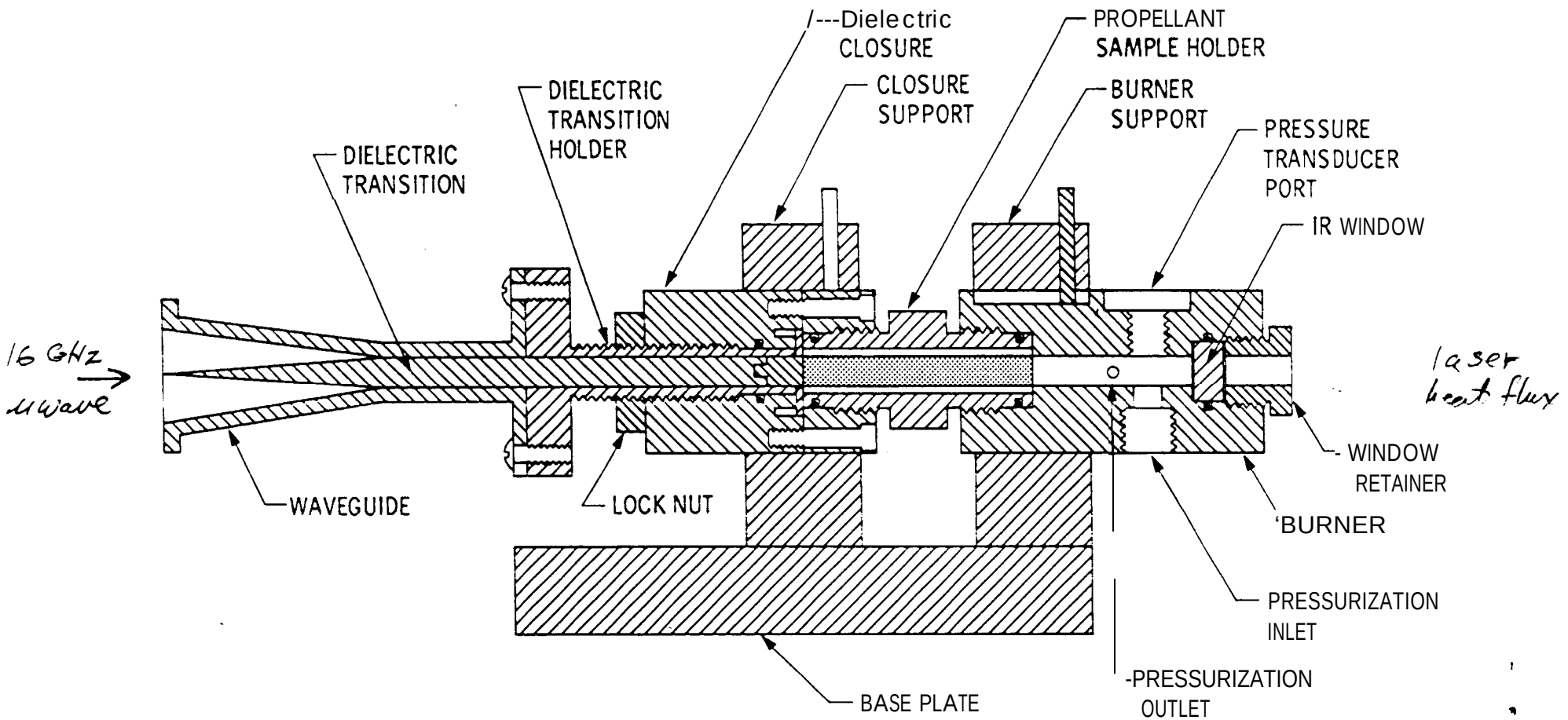

AIAA 89-2667

Test System

Microwave window burner and waveguide system

AIAA 89-2667

JPL DATA PROCESSING AND RECORDING SYSTEM

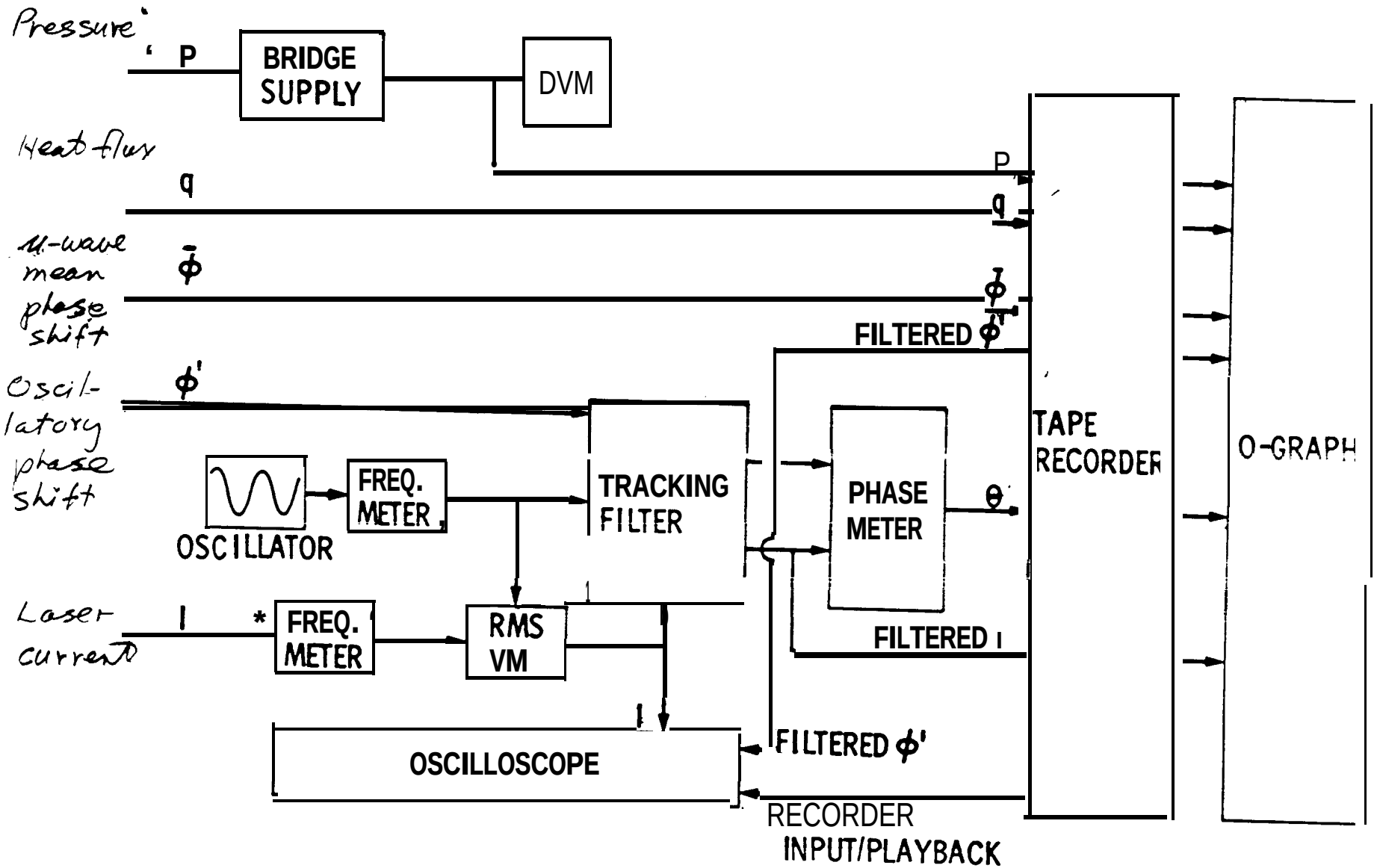

If in-depth transmission of the IR radiation (low absorption coefficient) were a factor, it would have to be included in the interpretive combustion model.

JPL

PROPELLANT IR RADIATION ABSORPTION CHARACTERISTICS

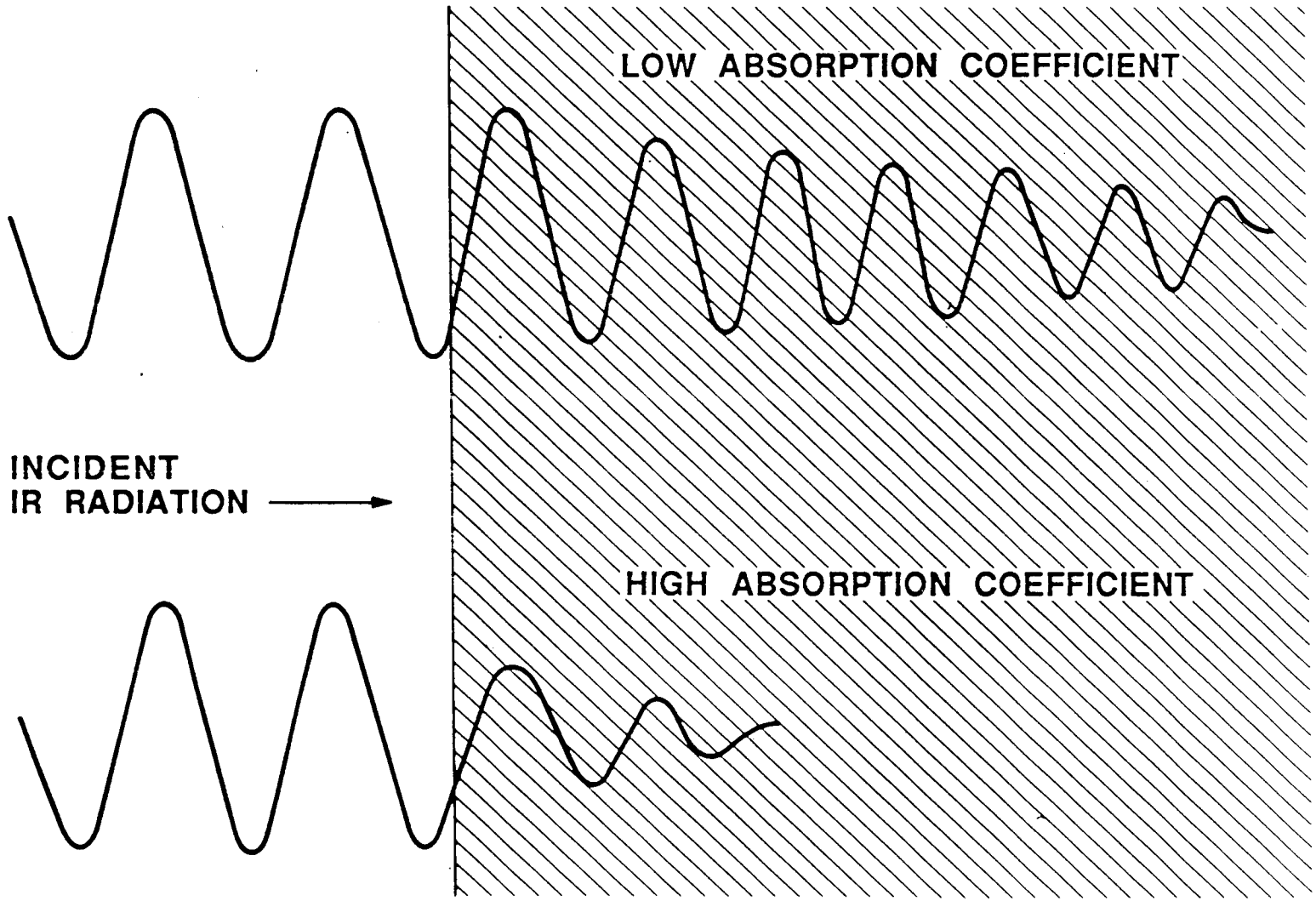

AIAA 89-2667

JPL

TEST PROPELLANT FORMULATIONS

	A-13 (control)	A-13, MOD. 1
AP (90 μm)	76.0%	75.75%
CARBON	0	0.25
PBAN-787	20.4	20.4
EPON RESIN 828	3.6	3.6

Added to increase IR radiation absorption coefficient

A-13 is a greater than 25 years old Navy propellant formulation that served as a JANNAF round robin test propellant and whose combustion response has been well characterized.

AIAA 89-2667

JPL

LASER MEAN HEAT FLUX vs FREQUENCY, A-13 TESTS

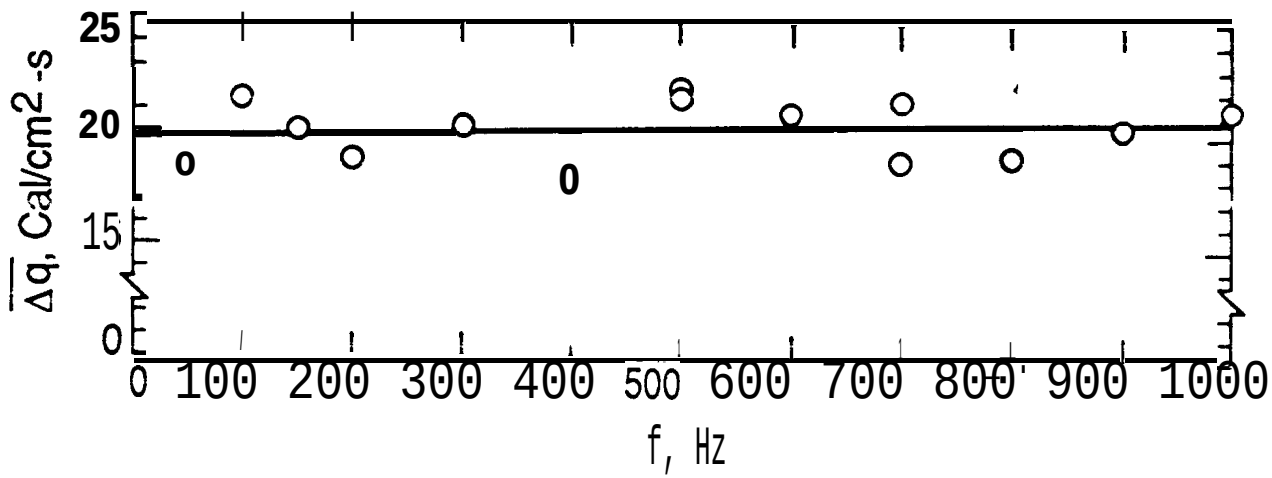

Measured variation in laser mean heat flux with frequency for the sinusoidally modulated CO_2 laser

AIAA 89-2667

JPL

LASER MEAN HEAT FLUX vs FREQUENCY, A-13, MOD. 1 TESTS

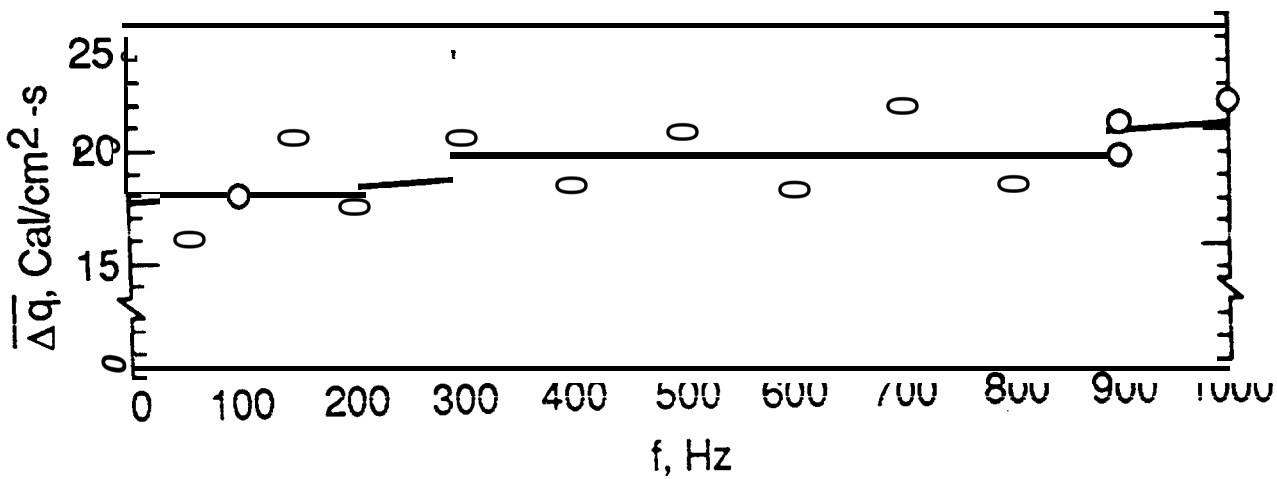

Results for second propellant test series

AIAA 89-2667

JPL OSCILLATORY PHASE SHIFT vs TIME

TEST 215-1 A-13 PROPELLANT

f □ 50 Hz, P = 300 Psia

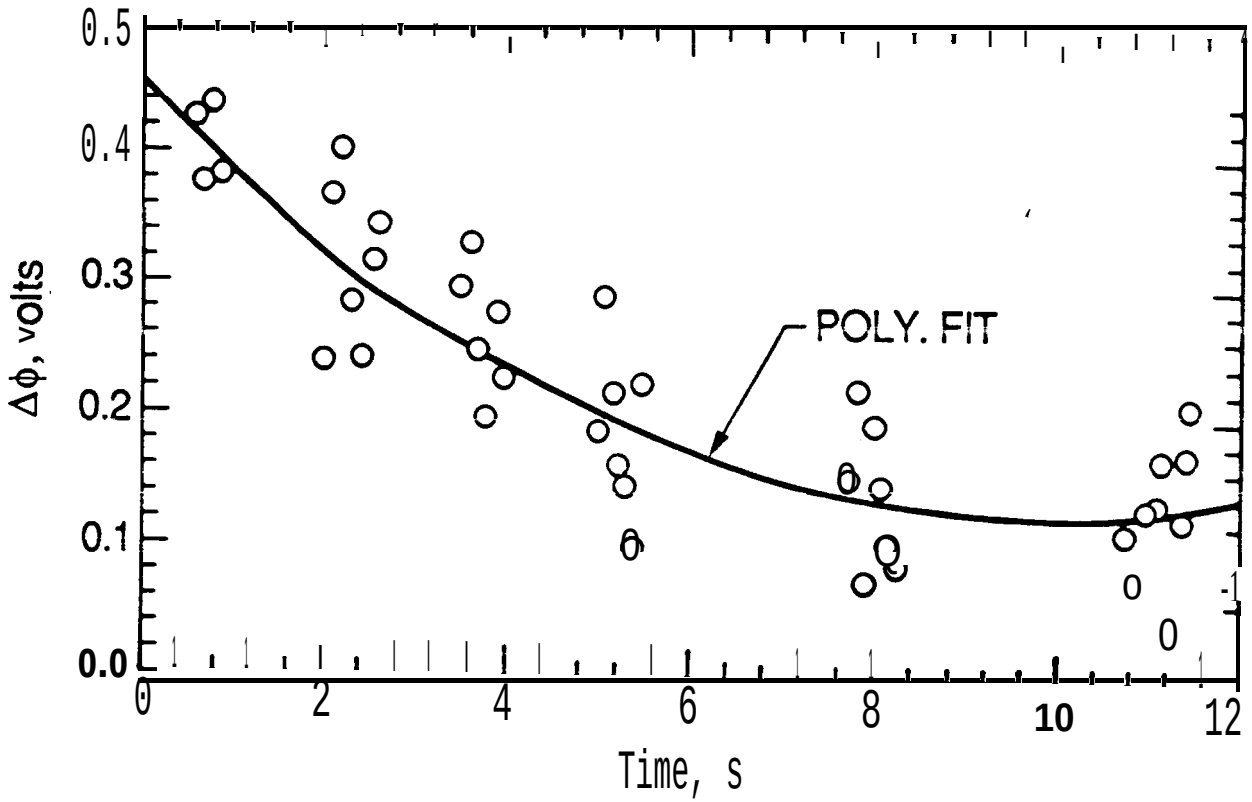

The reduction in Δφ amplitude with time is attributed to the attenuation of the radiant flux by the growing column of combustion gases in the propellant tube. The zero burn time intercept was taken as the non-attenuated value.

AIAA 89-2667

JPL OSCILLATORY PHASE SHIFT vs TIME

TEST 210-5 A-13, MOD. 1 PROPELLANT

f = 56 Hz, P = 300 Psia

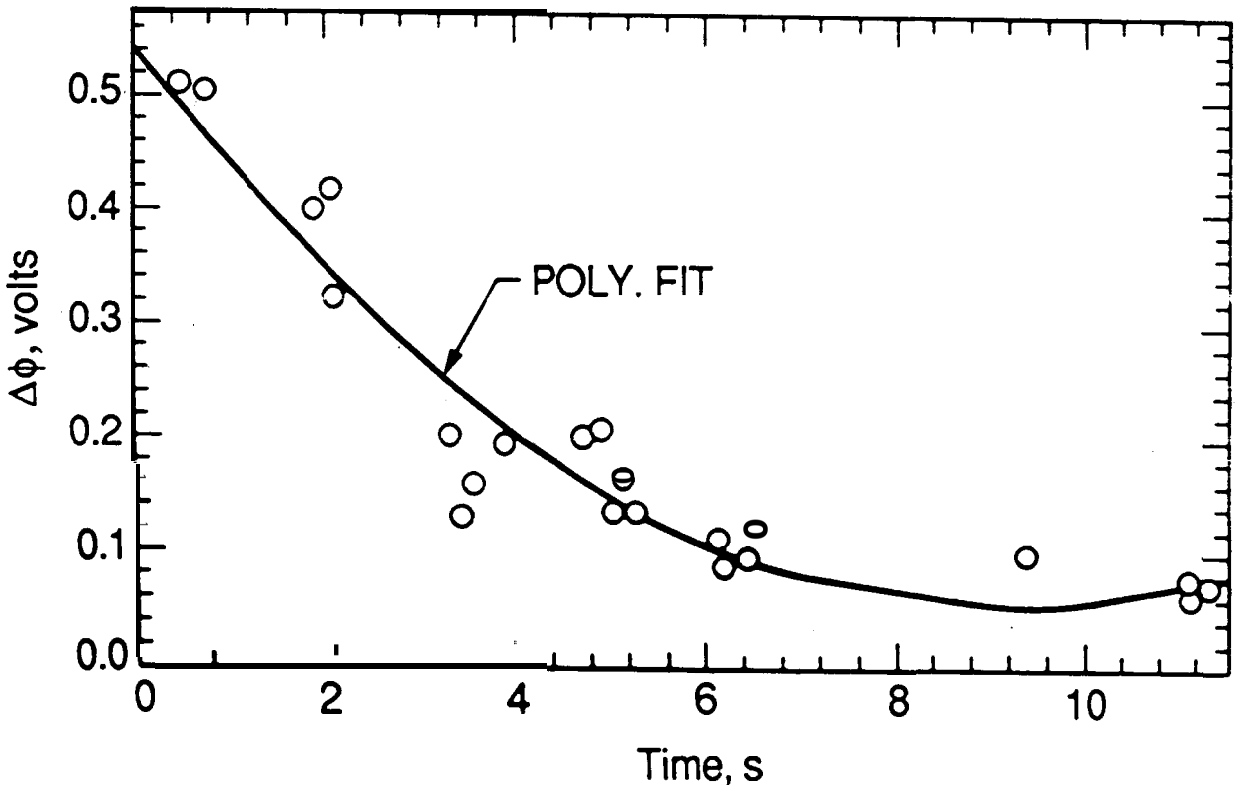

Second example

measured mean Doppler phase shift at a constant (continuous wave) heat flux. The zero time intercept was taken as the non-attenuated value.

AIAA 89-2667

JPL

RATE OF CHANGE OF DOPPLER PHASE SHIFT vs TIME, CONTINUOUS WAVE HEATING TEST

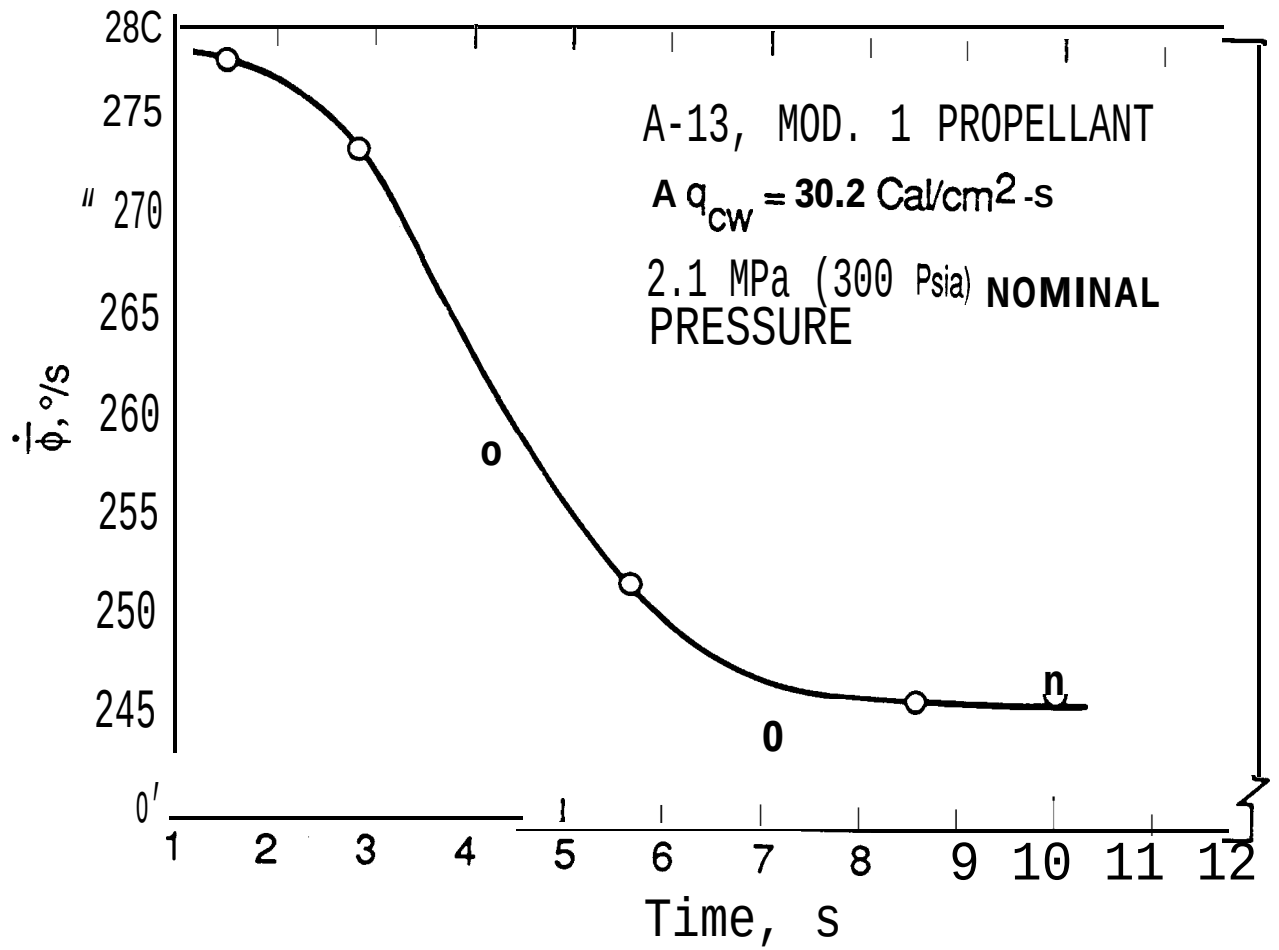

Determination of $\frac{\dot{\Phi}_{CW} - \dot{\Phi}_0}{\Delta q_{CW}}$ slope constant

AIAA 89-2667

JPL

RATE OF CHANGE OF DOPPLER PHASE SHIFT vs LASER CONTINUOUS WAVE HEAT FLUX, A-13, MOD. 1 PROPELLANT

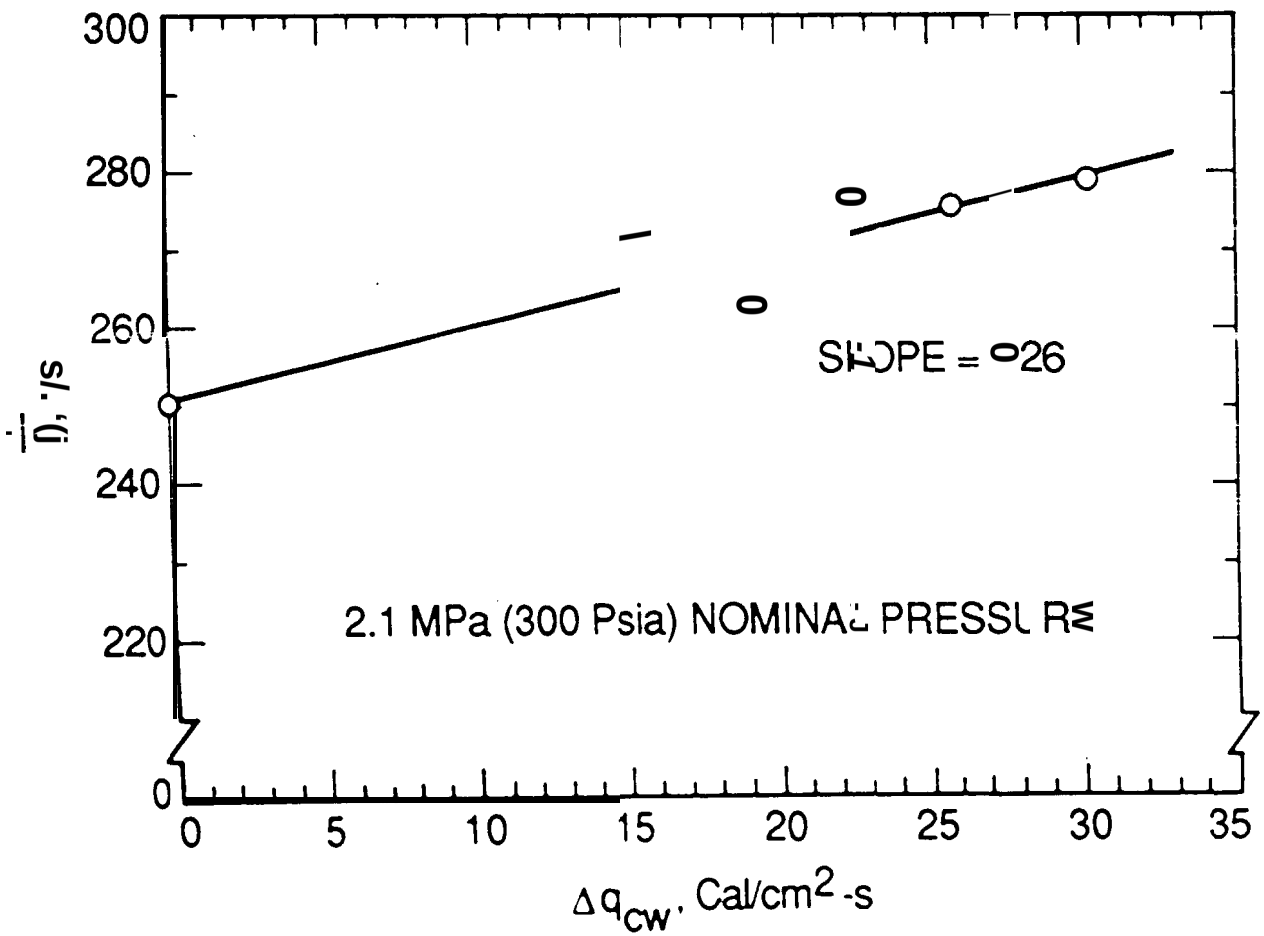

AIAA 89-
2667

JPL

ABSOLUTE VALUE OF OSCILLATORY RESPONSE vs FREQUENCY, A-13 PROPELLANT

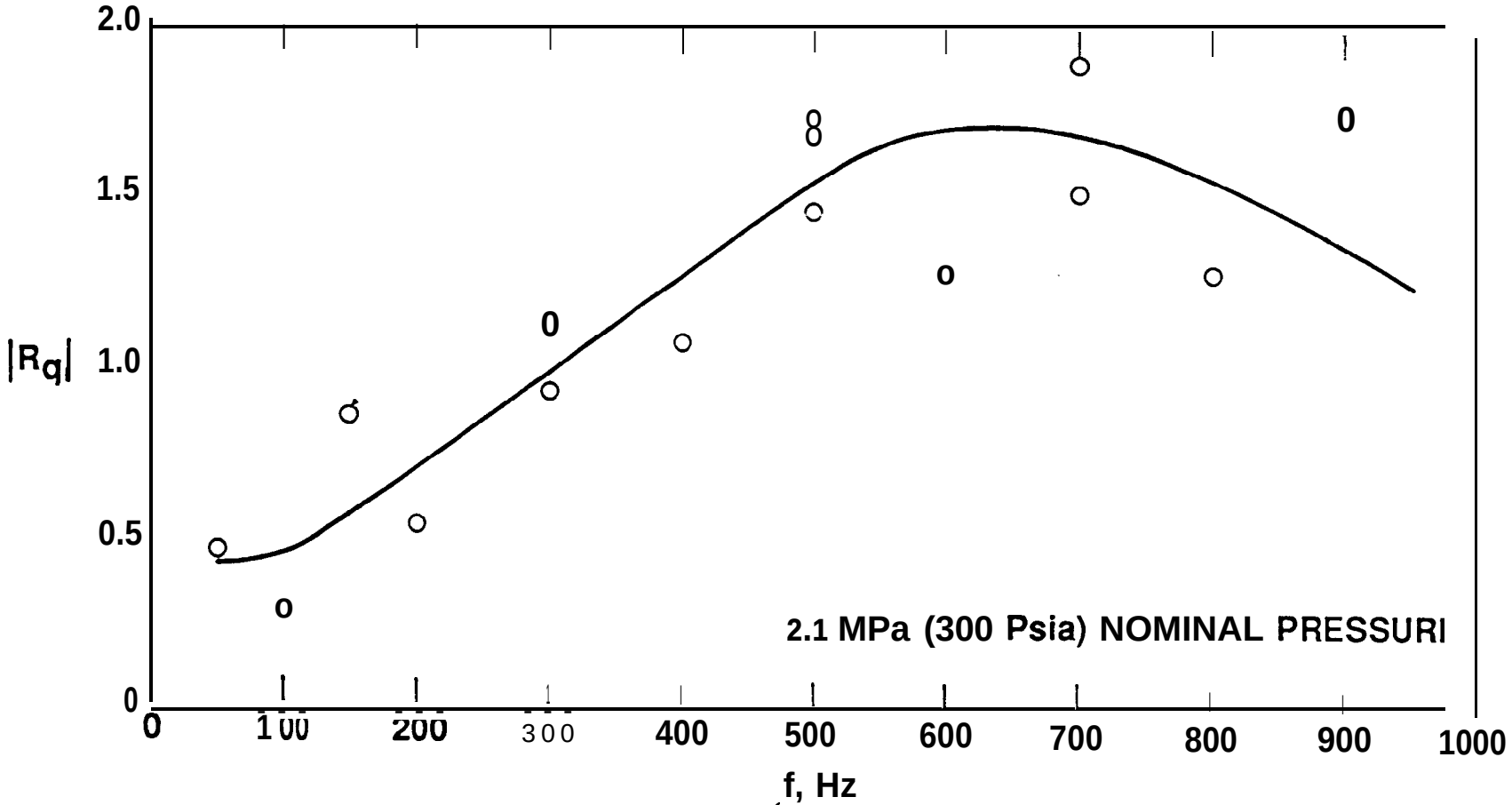

Laser modulation frequency

AIAA 89-2667

JPL

ABSOLUTE VALUE OF OSCILLATORY RESPONSE vs FREQUENCY, A-13, MOD. I PROPELLANT

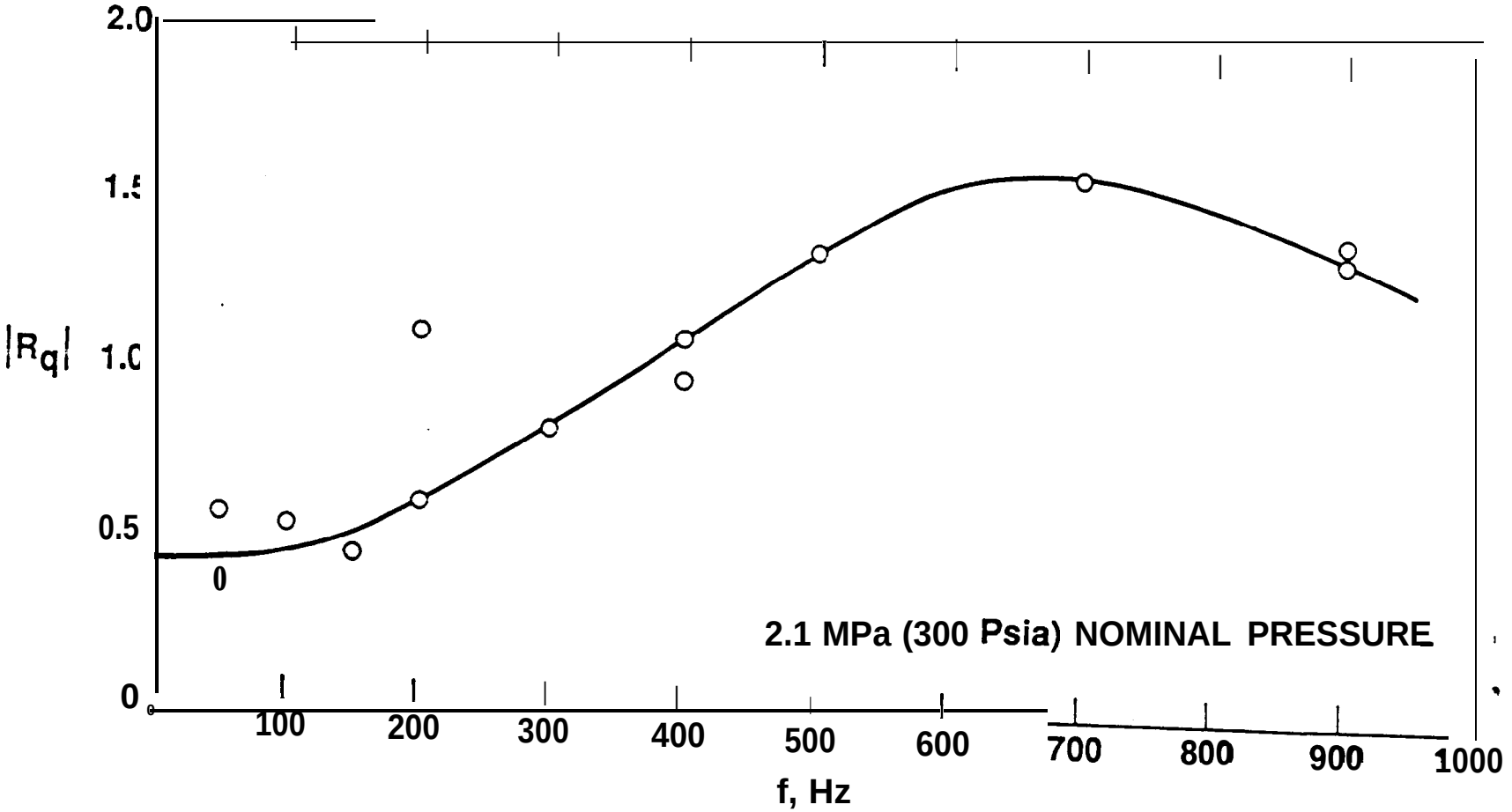

AIAA 89-2667

JPL

ARGUMENT OF OSCILLATORY RESPONSE vs FREQUENCY, A-13 PROPELLANT

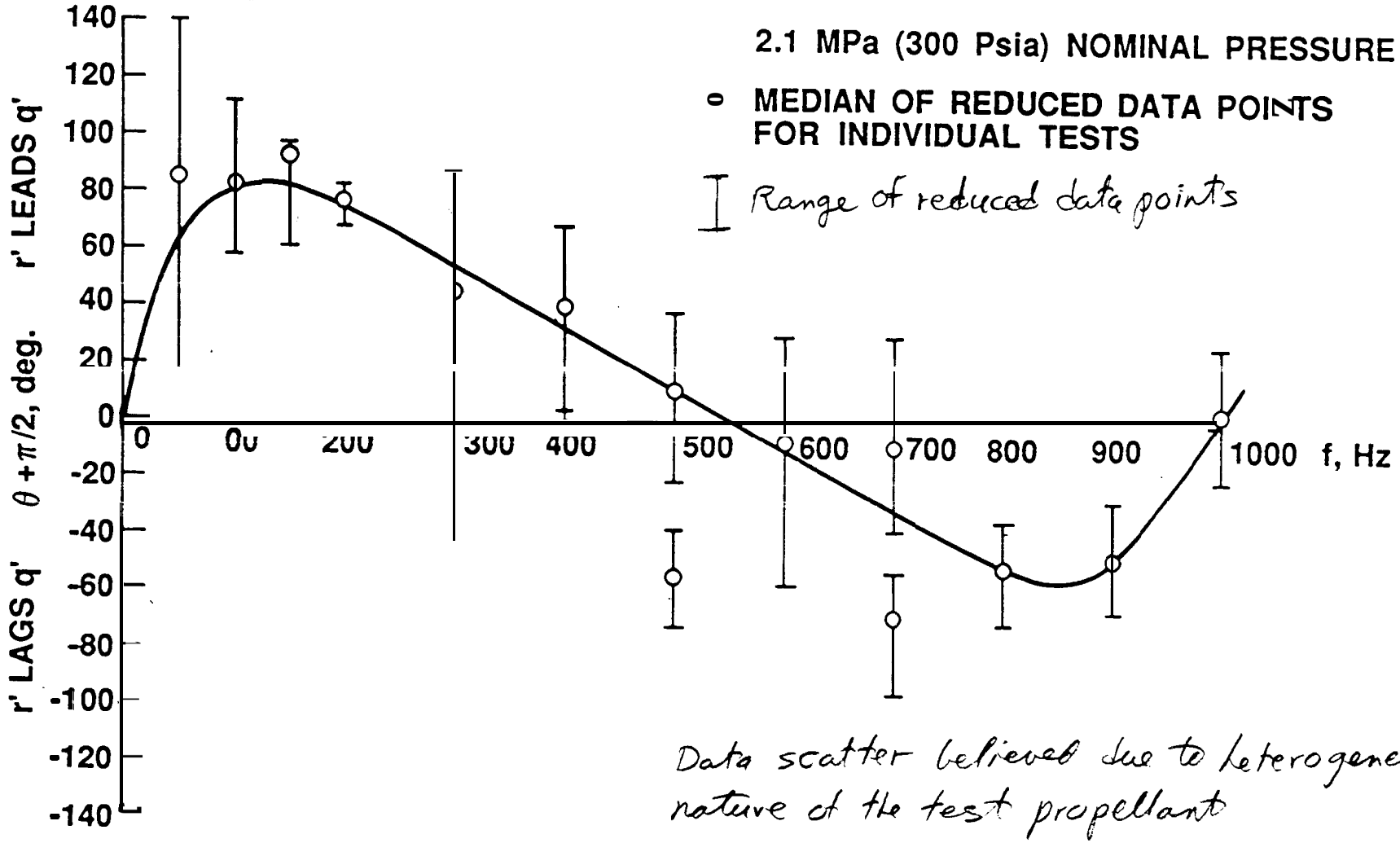

Data scatter believed due to heterogeneous nature of the test propellant

AIAA 89-2667

JPL

ARGUMENT OF OSCILLATORY RESPONSE *vs* FREQUENCY, A-13, MOD. 1 PROPELLANT

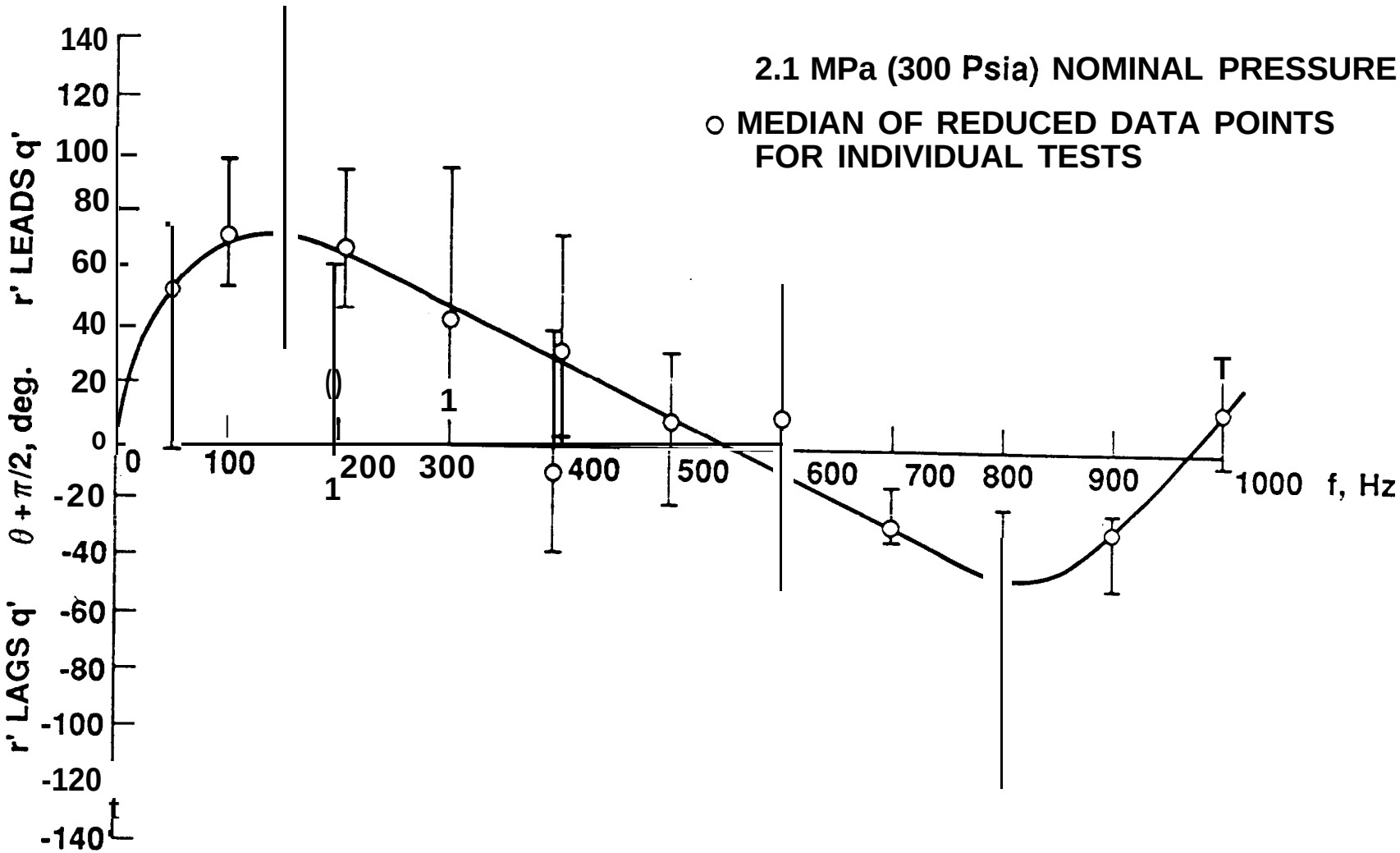

AIAA 89-2667

JPL REAL (IN-PHASE) COMPONENT OF OSCILLATORY RESPONSE vs FREQUENCY

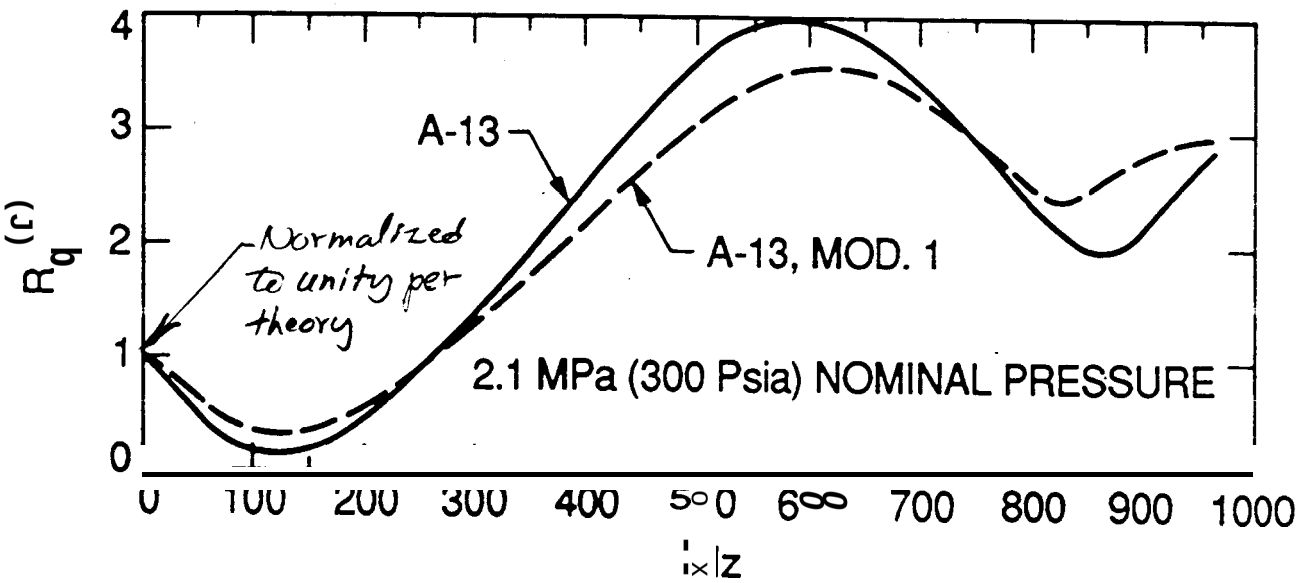

Product of curve fit to the $|R_q|$ data and the cosine of the curve fit to the argument data yields the real (in-phase) component

AIAA 89-2667

JPL REAL (IN-PHASE) COMPONENT OF PRESSURE-COUPLED RESPONSE FUNCTION vs FREQUENCY

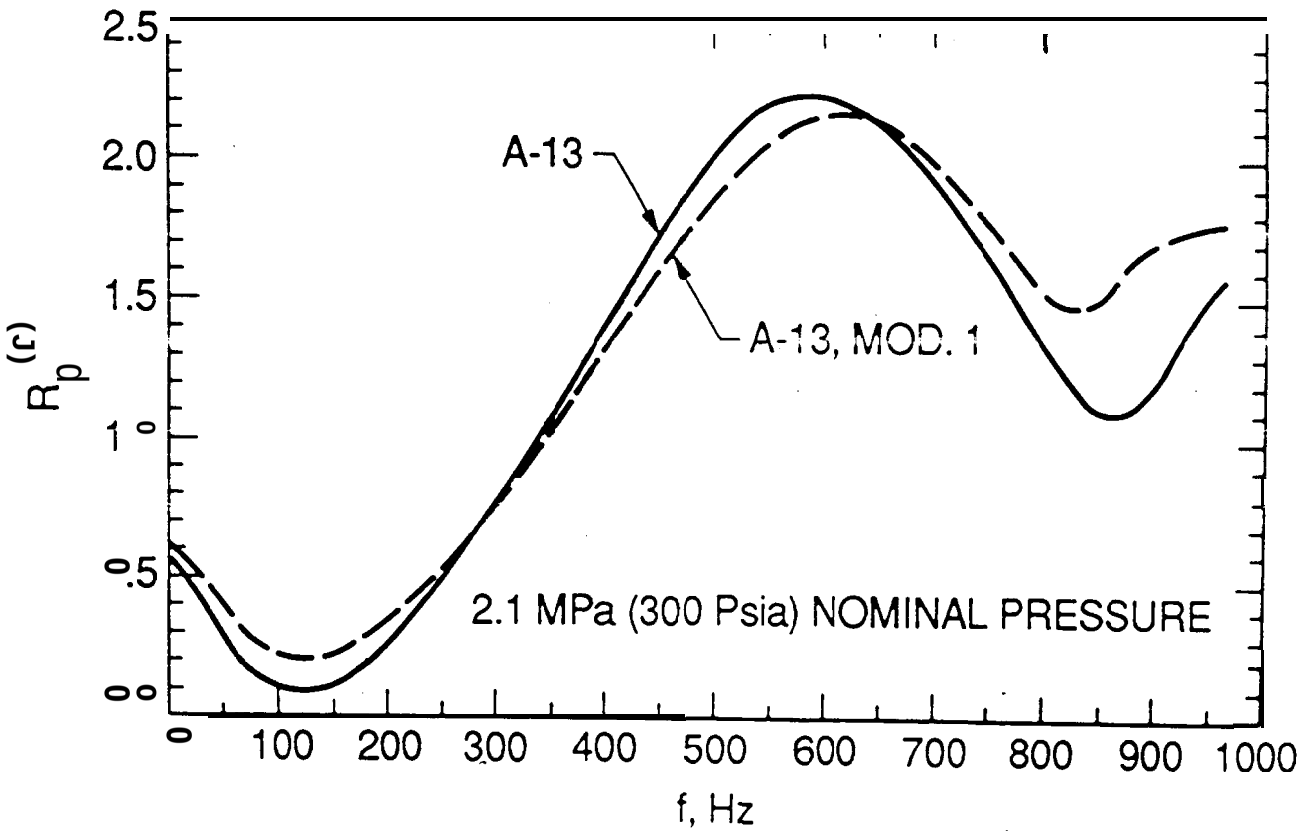

Real component of the pressure-coupled response function, obtained by multiplying the $R_q^{(r)}$ results by their respective transfer function, n. Differences for two test propellants concluded to be within experimental margin of error. ∴ in-depth heat transfer not factor.

AIAA 89-
2667

JPL REAL (IN-PHASE) COMPONENT OF PRESSURE-COUPLED RESPONSE FUNCTION vs FREQUENCY, A-13 PROPELLANT

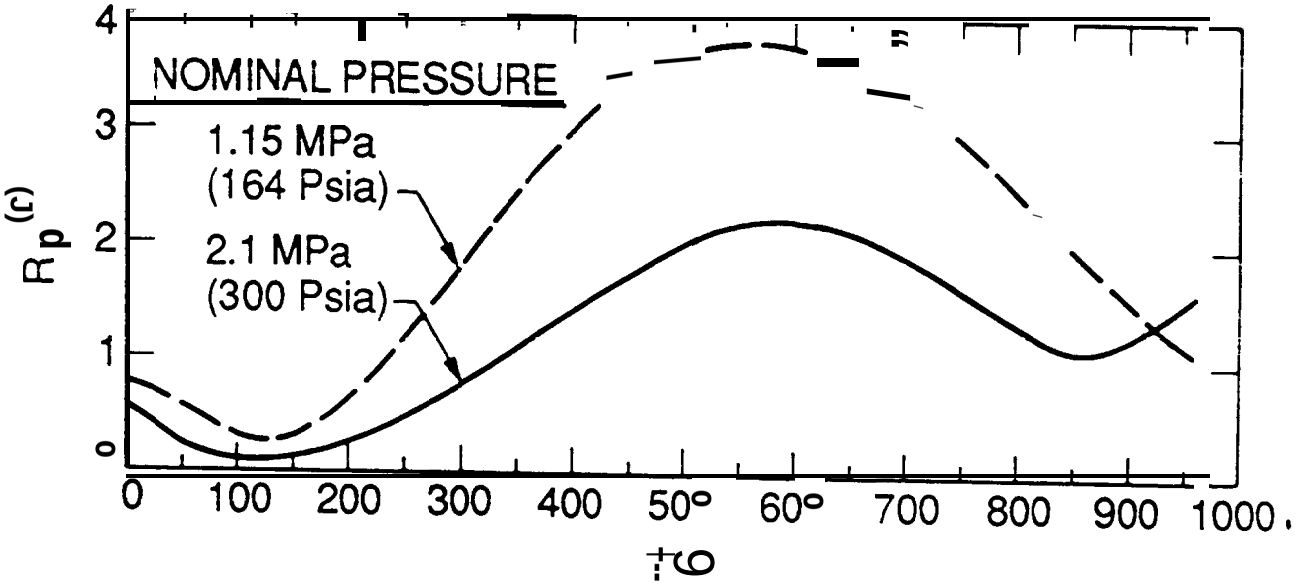

Pressure-coupled responses measured for two test pressures, showing increasing response with decreasing pressure - consistant with literature.

AIAA 89-2667

JPL

CONCLUSIONS

- MEASURED RESPONSE FUNCTION RESULTS FOR A-13 PROPELLANT FORMULATION (MAGNITUDE AND FREQUENCY RANGE OF MAXIMUM RESPONSE) COMPARABLE WITH EXISTING $R_p^{(r)}$ RESULTS OBTAINED BY A NUMBER OF DIFFERENT TECHNIQUES

- ADDITION OF QUARTER PERCENT CARBON HAD NO APPRECIABLE EFFECT ON MEASURED COMBUSTION RESPONSE CHARACTERISTICS - SUPPORTS CONCLUSION THAT IN-DEPTH TRANSMISSION OF RADIANT HEAT FLUX NOT A SIGNIFICANT FACTOR AT CO_2-LASER WAVELENGTH

- TESTS NEED TO BE PERFORMED ON HOMOGENEOUS PROPELLANTS TO DETERMINE VALIDITY OF POSTULATED REASON FOR LARGE TIME-VARIATION IN RESPONSE FUNCTION ARGUMENT DATA

- TECHNIQUE SHOWS PROMISE AS A TOOL FOR CHARACTERIZING PROPELLANT COMBUSTION STABILITY

Results of test series on high burning rate (~ 2 in./s at 2000 psia) igniter propellant

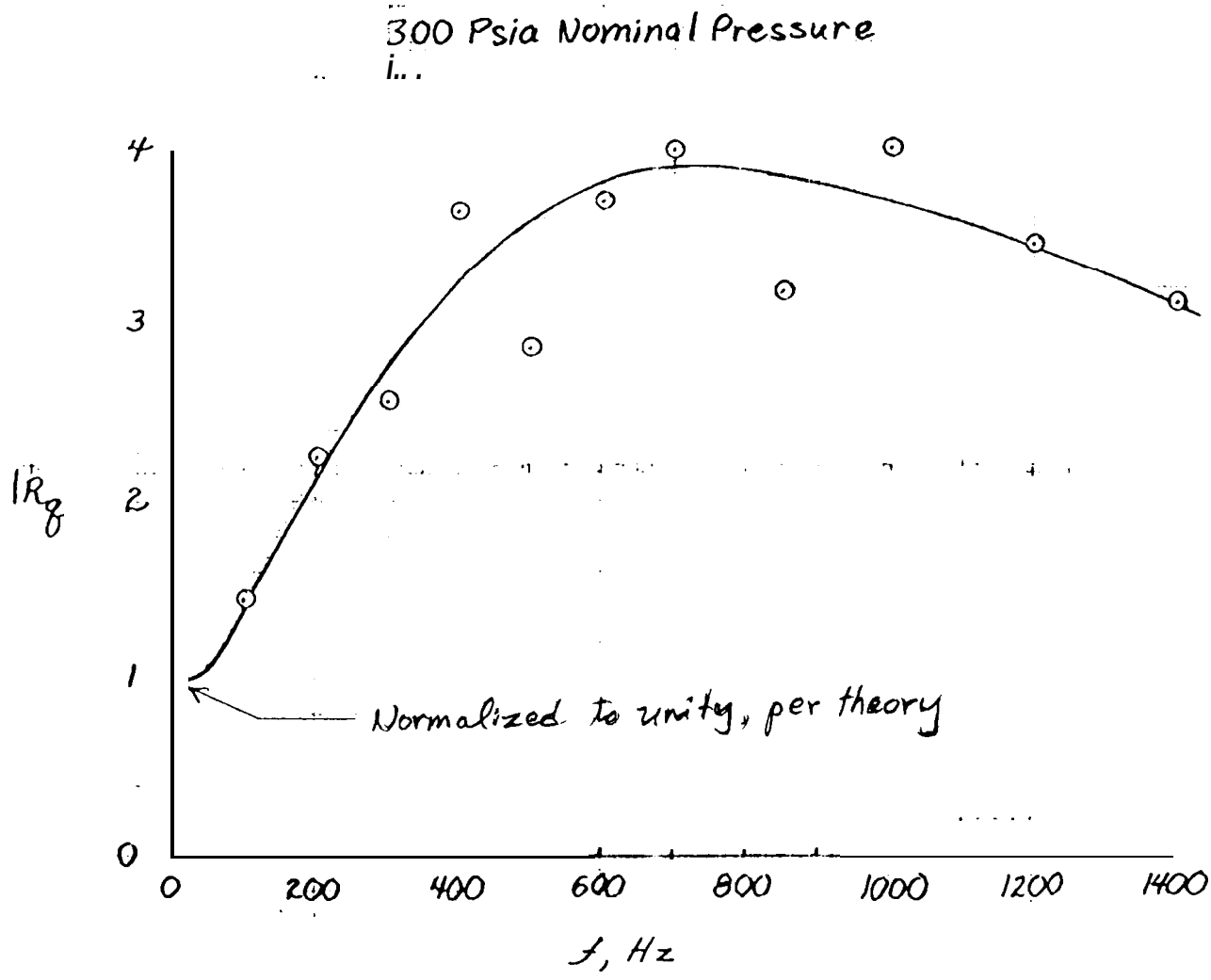

Figure 9 Absolute value of heat flux response function vs. frequency for ASRM Igniter Propellant

Feb. 1992 report to NASA MSFC

DIETZGEN CORPORATION
MADE IN U.S.A.

For this propellant the dynamic burning rate, r', leads the oscillatory heat flux driver, q', over the frequency range of 300 to 1500 Hz.

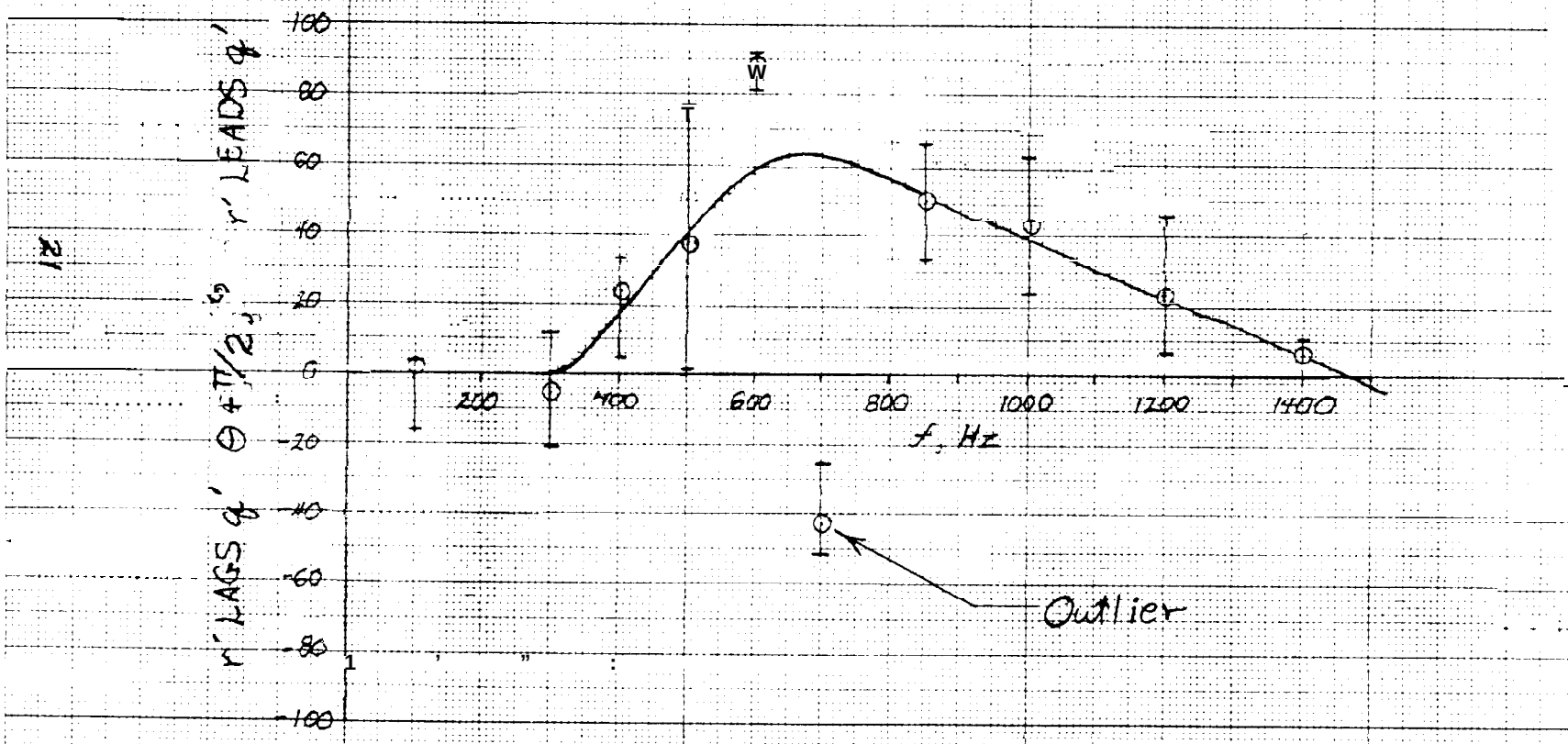

Figure 10. Argument of response function vs. frequency for ASRM Igniter propellant

Feb. 1992 report to NASA MSFC

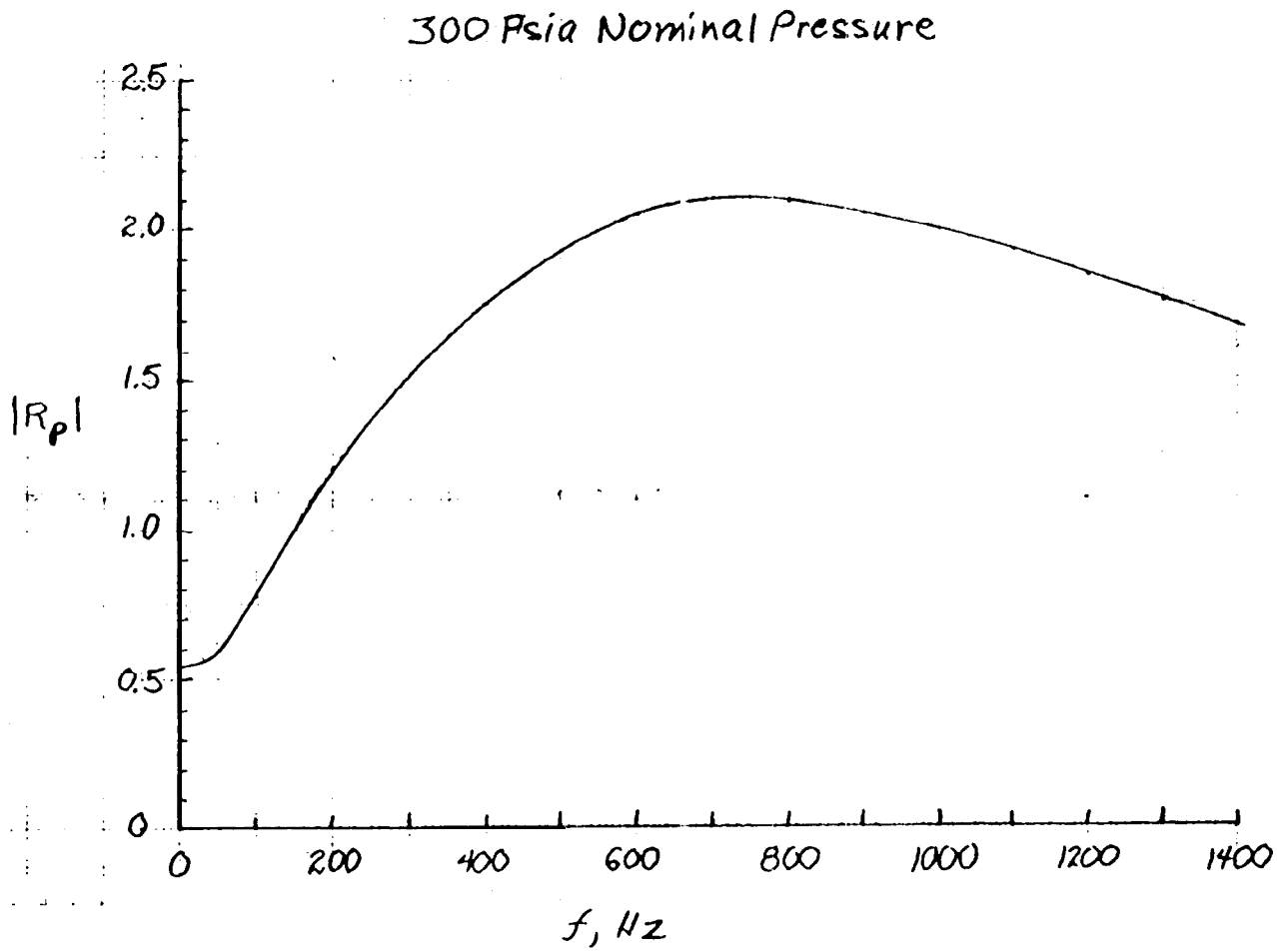

Figure 11. Absolute value of pressure-coupled response function vs. frequency for ASRM Igniter propellant

Determined by multiplying the curve fit to the $|R_q|$ data by the propellant's burning rate pressure exponent, n.

Normalizing the test results by plotting versus frequency over burning rate squared in an attempt to apply the results to pressures other than the 300 psia test pressure

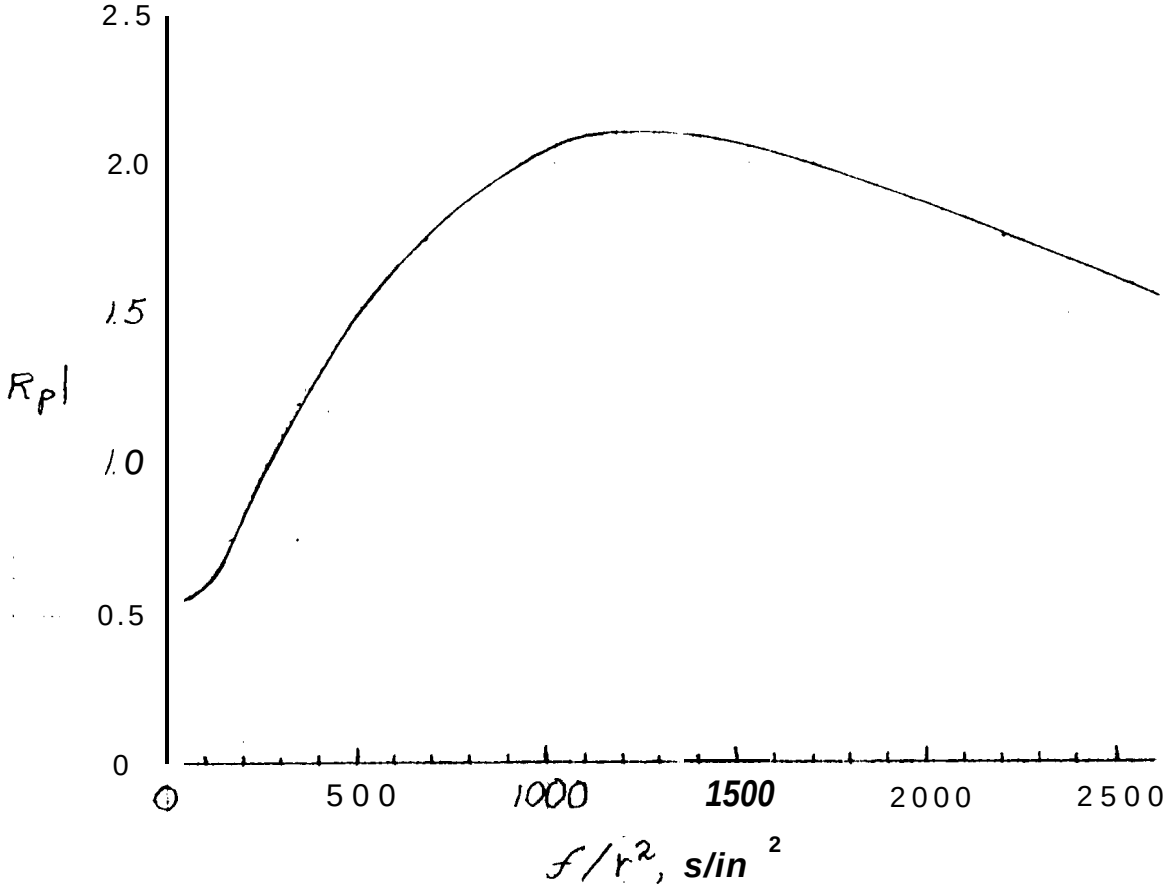

Figure 12.- Absolute value of pressure-coupled response function vs. normalized frequency for ASRM Igniter Propellant

Real component obtained by taking the product of the $|R_p|$ curve and the cosine of the curve fit to the argument data, $\Theta + \pi/2$. The argument results produce a characteristic bimodal response, with peaks at frequencies of 400 and approximately 1250 Hz (at this test pressure).

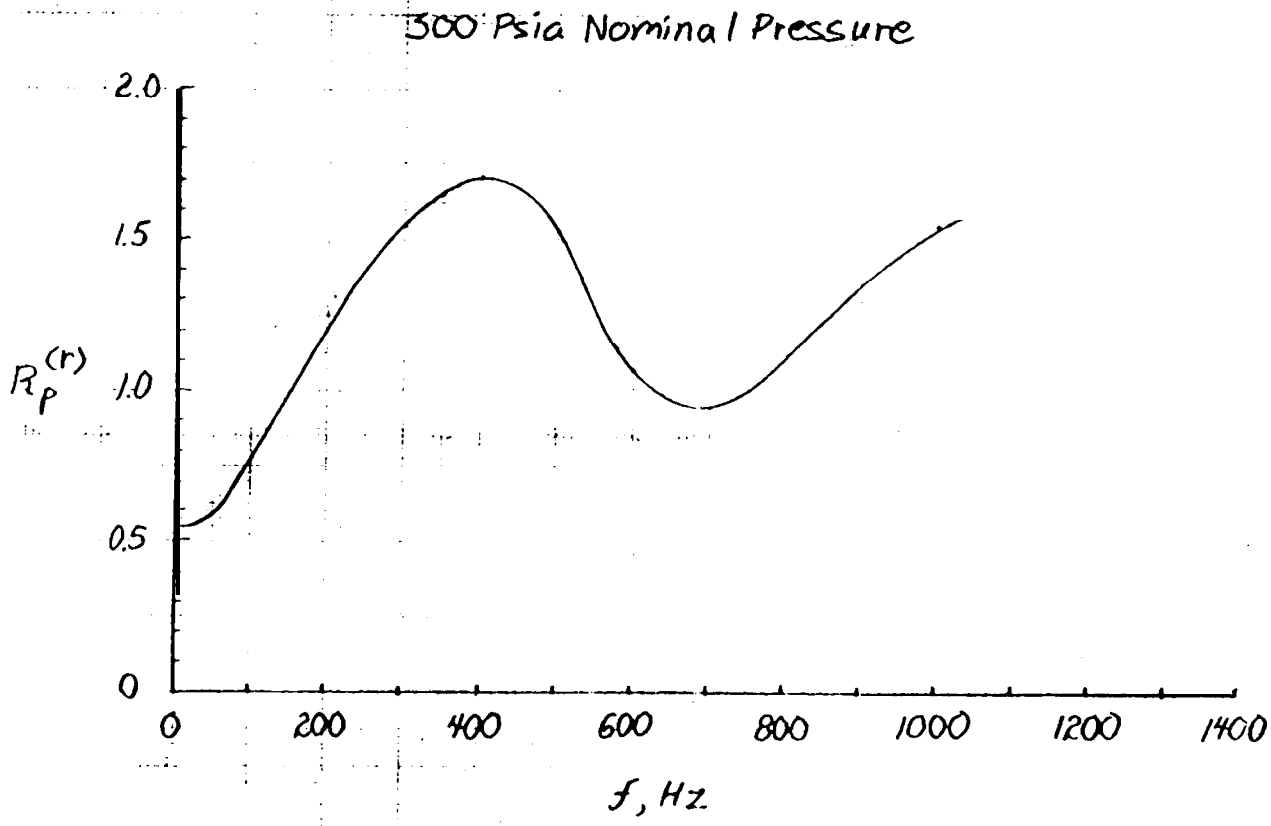

Figure 13. Real component of pressure-coupled response function vs. frequency for ASRM Igniter propellant

Feb. 1992 report to NASA MSFC

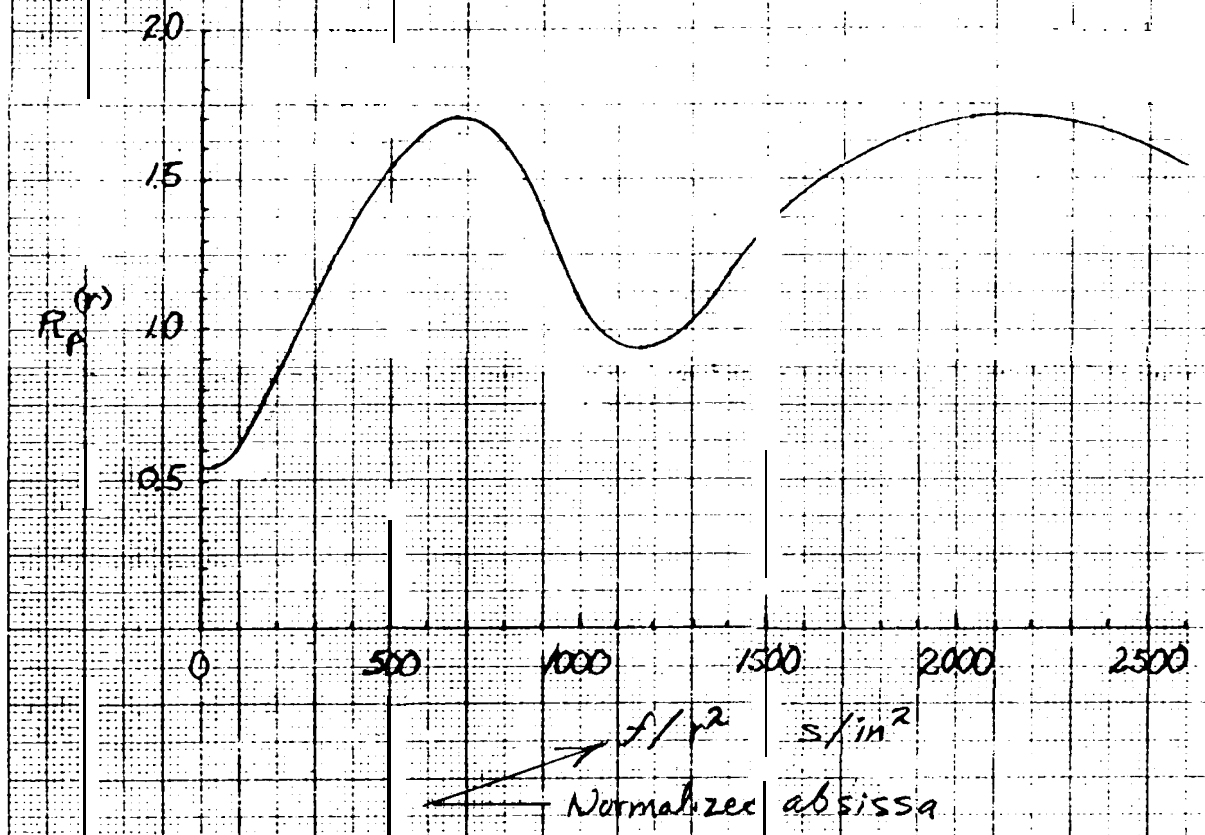

Figure 14. Real component of pressure-coupled response function vs frequency for ASRM Igniter Propellant

For any operating pressure, the frequencies of peak response can be estimated by multiplying the respective f/r^2 value by the square of the burning rate at that pressure.

PLASMA CAPACITANCE GAGE PROPELLANT BURNING RATE MEASUREMENT TECHNIQUE

Definition of erosive burning in solid propellant rocket motors

JPL

EROSIVE BURNING

- THE AUGMENTATION IN BURNING RATE OF SOLID PROPELLANTS PRODUCED UNDER CONDITIONS OF HIGH-SPEED FLOW PARALLEL TO PROPELLANT BURNING SURFACE.

- PREDICTED TO BE ENHANCED BY FACTORS THAT INCREASE LEVEL OF TURBULENCE CLOSE TO PROPELLANT BURNING SURFACE.

  - HIGH CROSS-FLOW VELOCITY.

  - LOW SURFACE BLOWING RATE (LOW PROPELLANT BURNING RATE, HIGH CHAMBER PRESSURE).

  - PROPELLANT SURFACE ROUGHNESS.

DESCRIPTION OF JPL

JPL" "

EROSIVE BURNING RESEARCH

• PURPOSE

- TO MEASURE EFFECTS OF PARAMETERS THAT ARE CONSIDERED TO MOST STRONGLY INFLUENCE SCALING TO LARGER ROCKET MOTOR SIZES OF TRANSITION OR THRESHOLD CONDITIONS FOR EROSIVE BURNING RATE AUGMENTATION
- DEVELOP A SCALING CRITERION FOR THRESHOLD CONDITIONS FOR EROSIVE BURNING

'APPROACH

- CARRY OUT SERIES OF LARGE-SCALE MOTOR FIRINGS SYSTEMATICALLY VARYING (1) MOTOR CROSS-FLOW VELOCITY OR MACH No., (2) CHAMBER PRESSURE, (3)-PROPELLANT NON-EROSIVE BURNING RATE, (4) -PROPELLANT SURFACE ROUGHNESS, AND-(5) MOTOR PORT DIAMETER, AND MEASURING MOTOR TRANSITION LENGTH TO EROSIVE BURNING RATE AUGMENTATION
- INCORPORATE EROSIVE BURNING DEPENDENCIES ON TEST PARAMETERS INTO SCALING CRITERION

Measured erosive augmentation of propellant base burning rate (r/r_0) using plasma capacitance gage technique.

r_0 = propellant base burning rate without crossflow of combustion gases

AIAA 90-2327

Instrumented Solid Propellant Rocket Motor

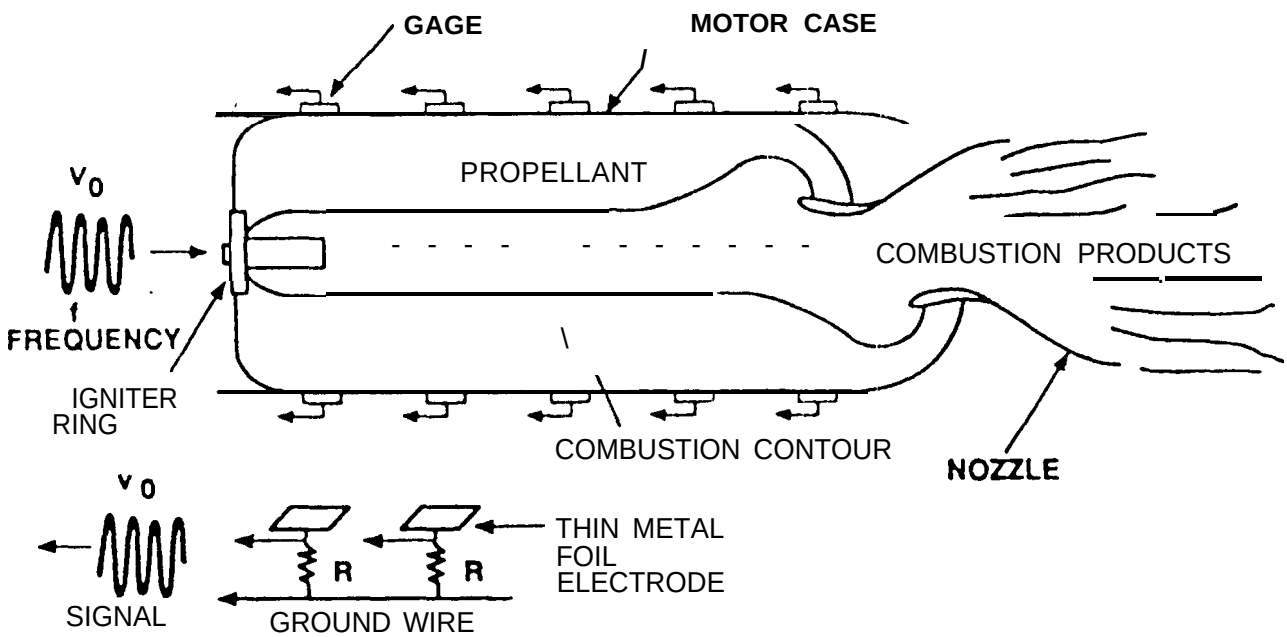

Figure 1. Plasma Capacitance Gage-Principle of Operation

Each PCG consists of a capacitor formed between an electrode located at the outer surface of the propellant grain and the ionized flame zone (as ground), with the propellant web as the capacitor dielectric. The changing capacitance with regression of the burning surface, input into an analytical model of the device, yields a continuous measurement with time of the local propellant web thickness and consequently burning rate.

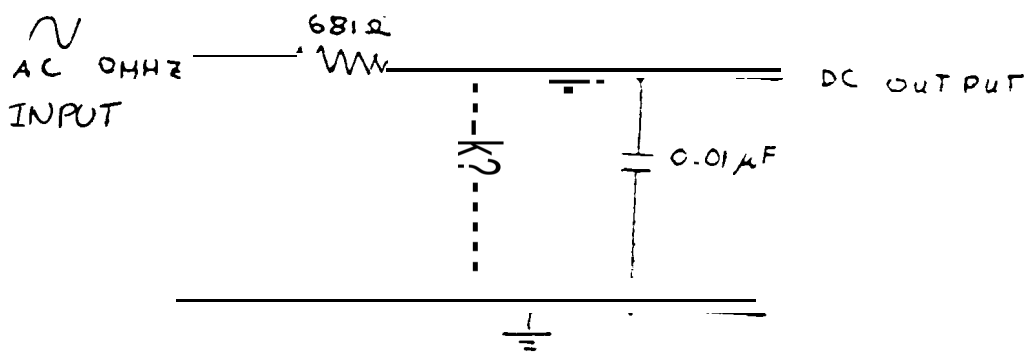

FIG 2 Plasma Capacitance Gage Electronics

Each gage circuit is a resistor to capacitor AC voltage divider with two rectifier diodes and a filter capacitor.

AIAA 89-2528

JPL BATES EROSIVE BURNING TEST MOTOR

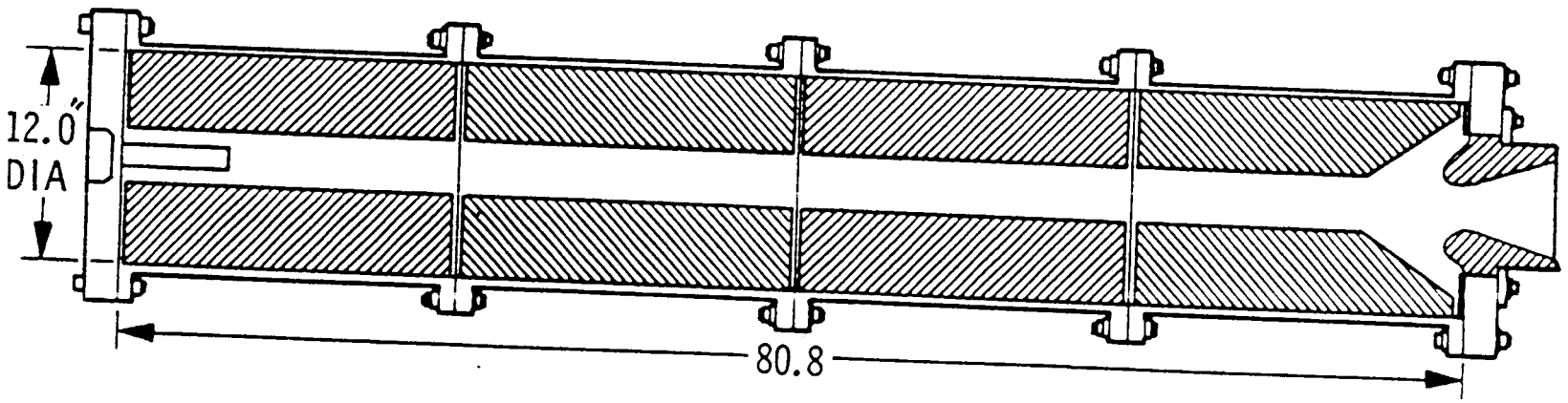

AIAA-88-3254

BATES EROSIVE BURNING TEST MOTOR

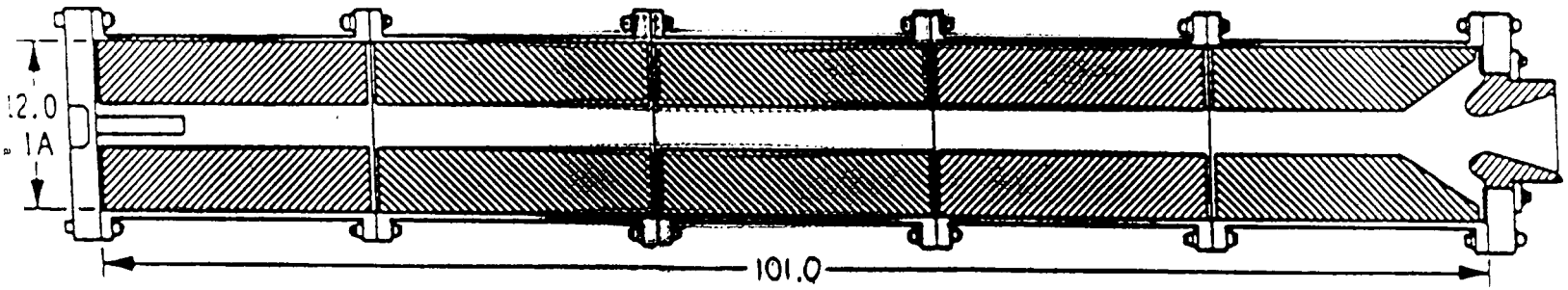

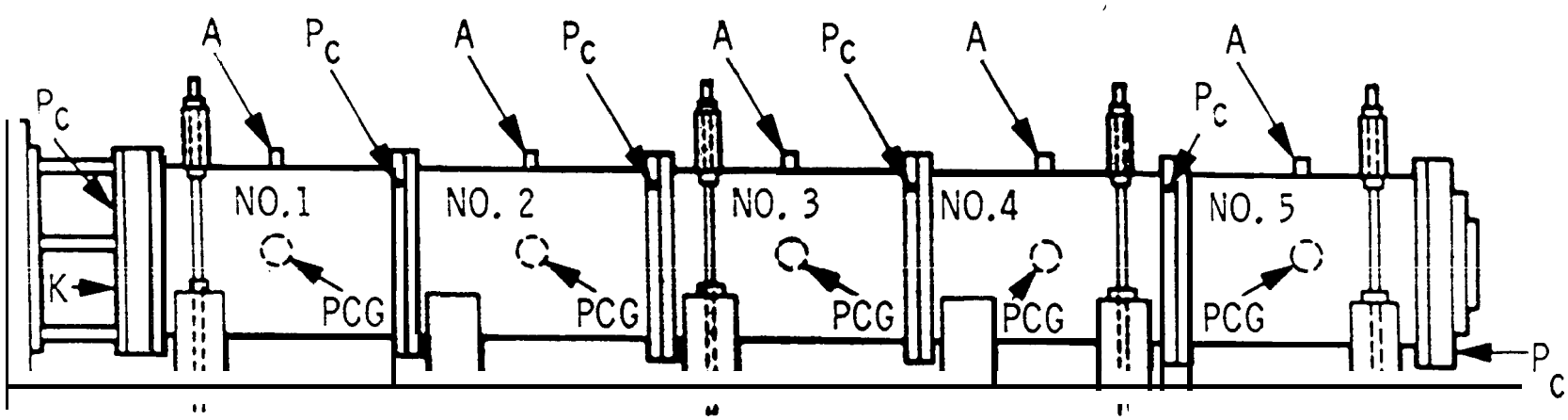

A ACCELEROMETER
P_C CHAMBER PRESSURE TRANSDUCER
PCG PLASMA CAPACITANCE GAUGE
K KISTLER PRESSURE TRANSDUCER

CPIA Publ. No. 432 12 inch (BATES) rocket motor segment instrumented with plasma capacitance gage electrode

JPL

INTERMEDIATE SEGMENTS

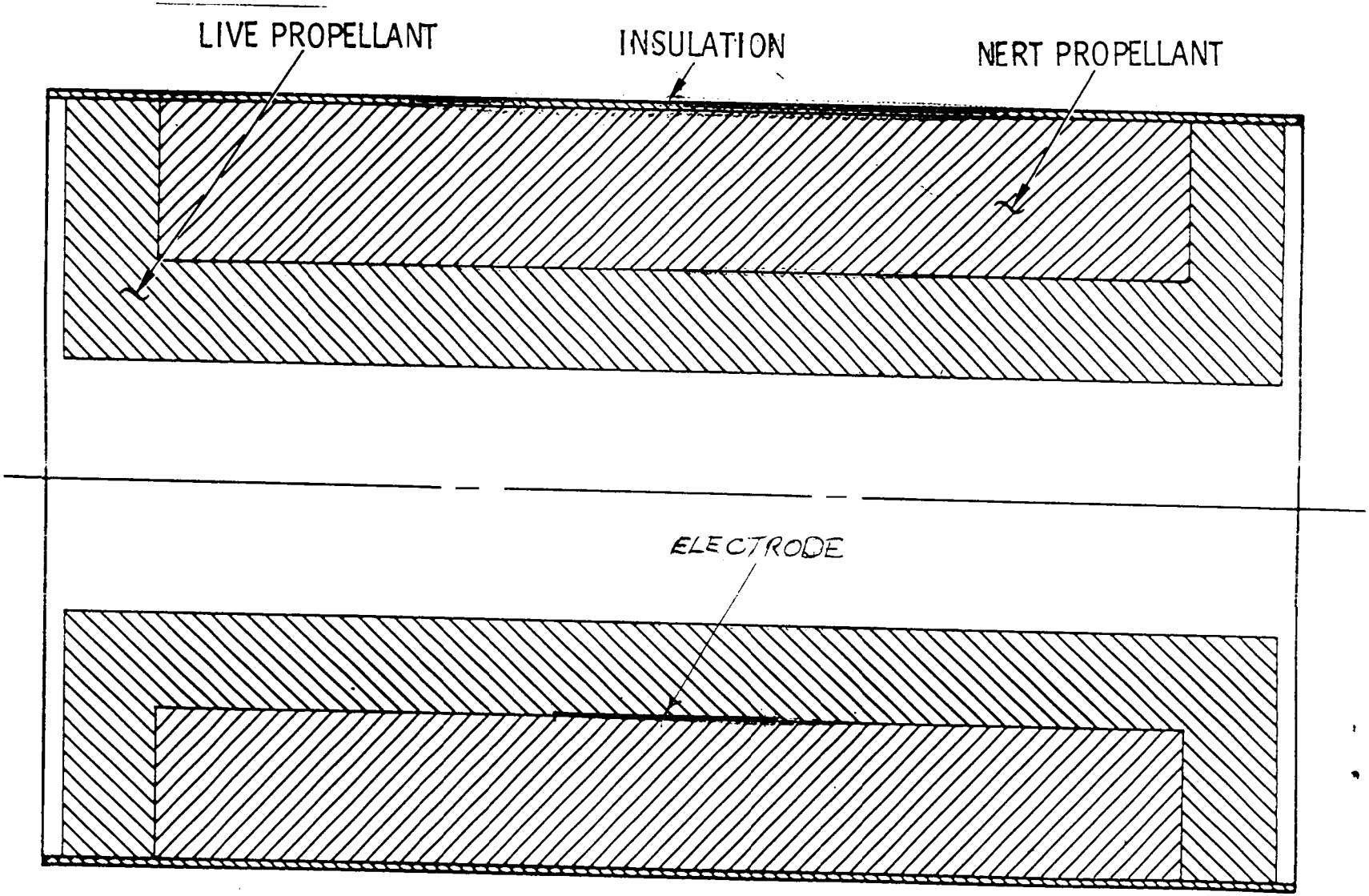

AIAA 89-2528

JPL SEGMENTED 5 × 1° IN. BATCH-CHECK CHAMBERS

TEST MOTOR

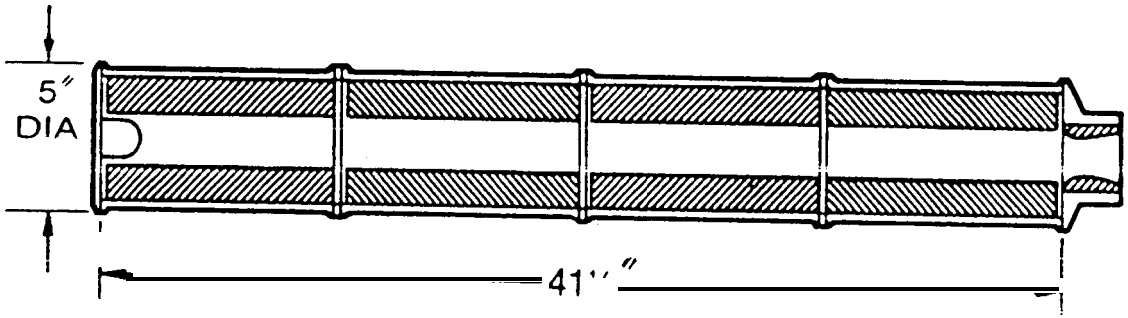

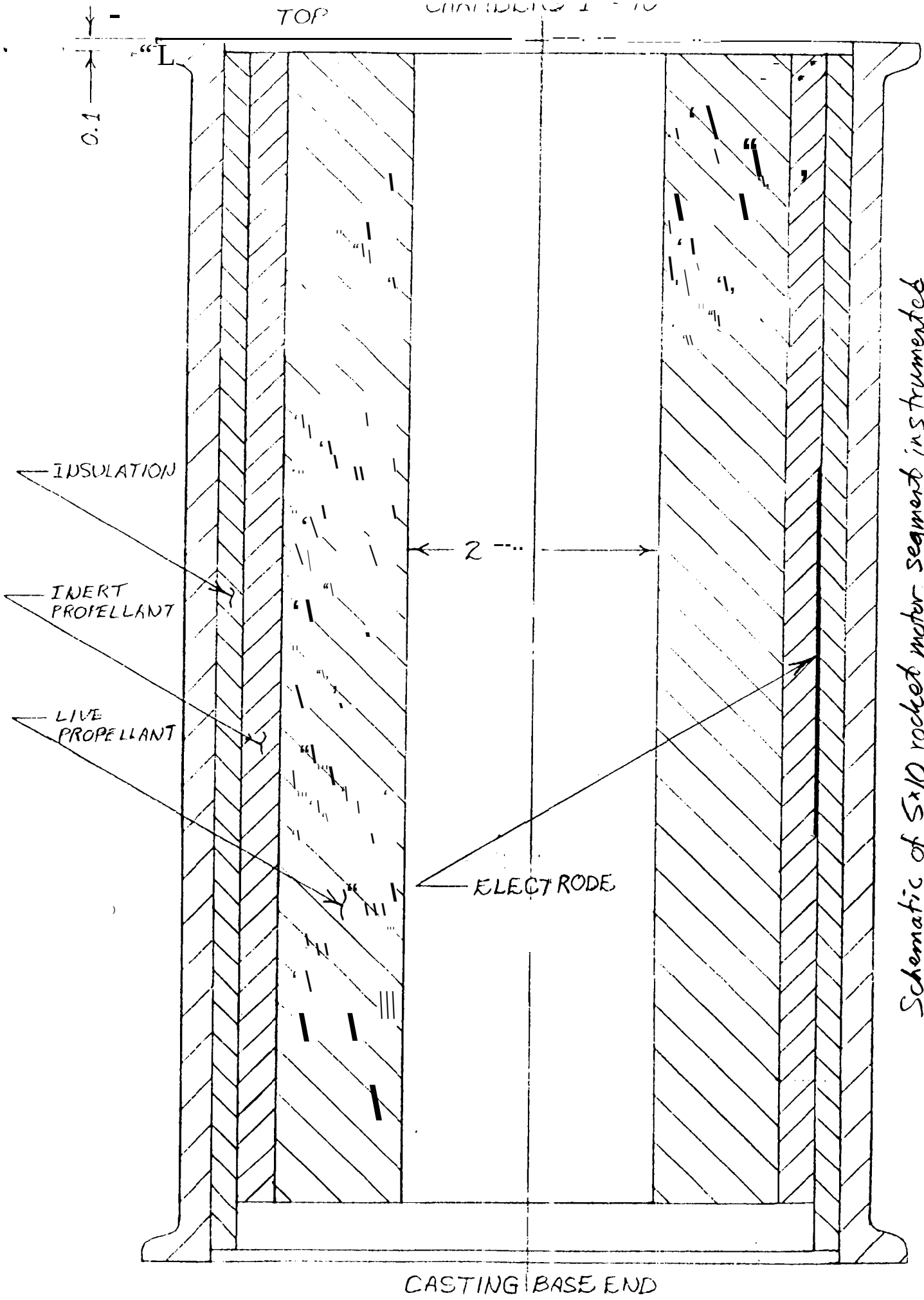

Schematic of 5x10 rocket motor segment instrumented with plasma capacitance gage electrode.

JOL

CHAMBER PRESSURE vs TIME

TEST NO. 10, 5 x 10 MOTOR

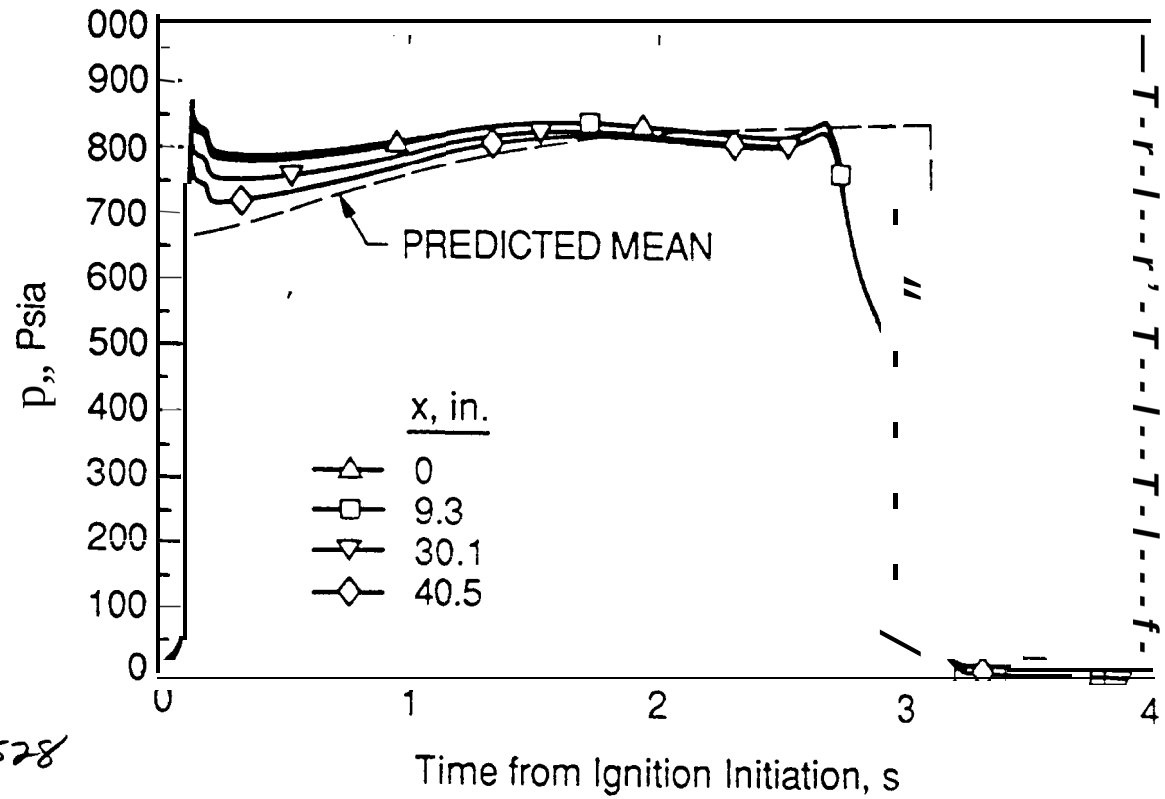

AIAA 89-2528

Plot of the mean pressure at axial measurement stations along the rocket motor for a typical 5x10 segmented motor test, showing the higher than predicted initial pressure caused by the erosive burning-rate augmentation and an axial pressure gradient down the motor port that diminishes with time (increasing port diameter).

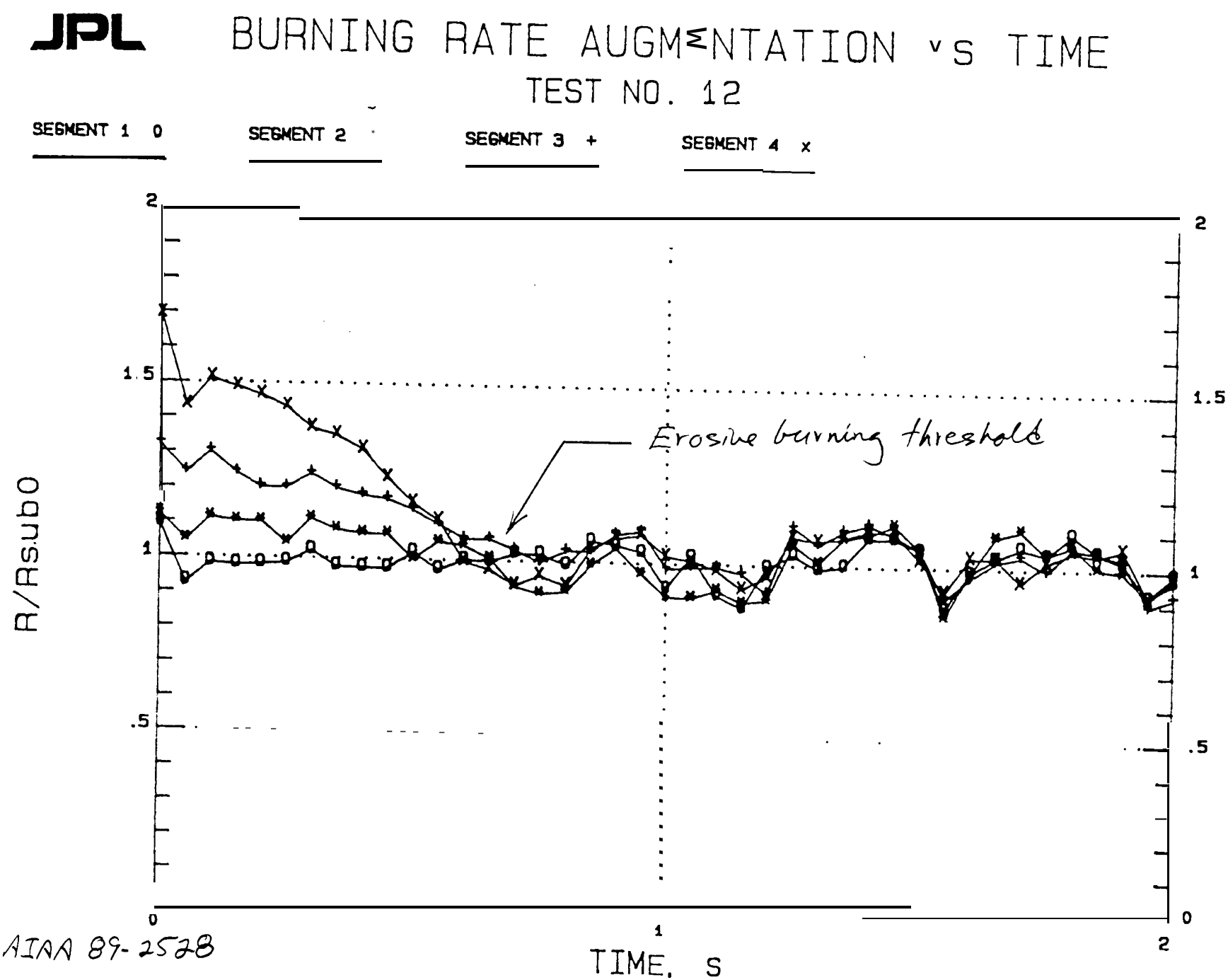

AIAA 89-2528

Example of measured burning rate results, normalized by the strand burner, no-crossflow rates at the corresponding pressures, for four segment 5x10 motor test

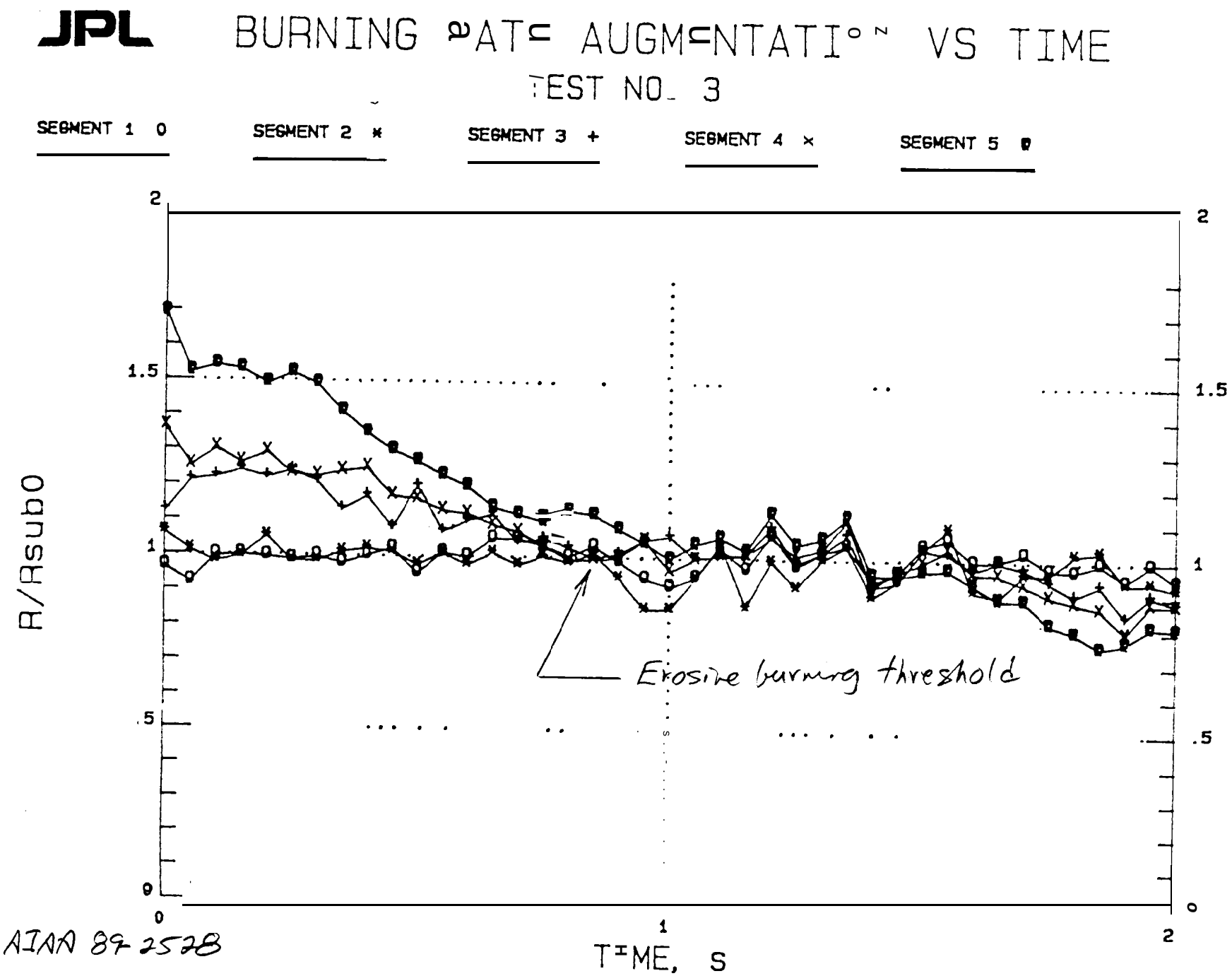

AIAA 89-2528

Example of measured burning rate results, normalized by the no-crossflow rates, for a five segment 5X10 motor test

BURNING RATE AUGMENTATION vs TIME

TEST N°. E-1923

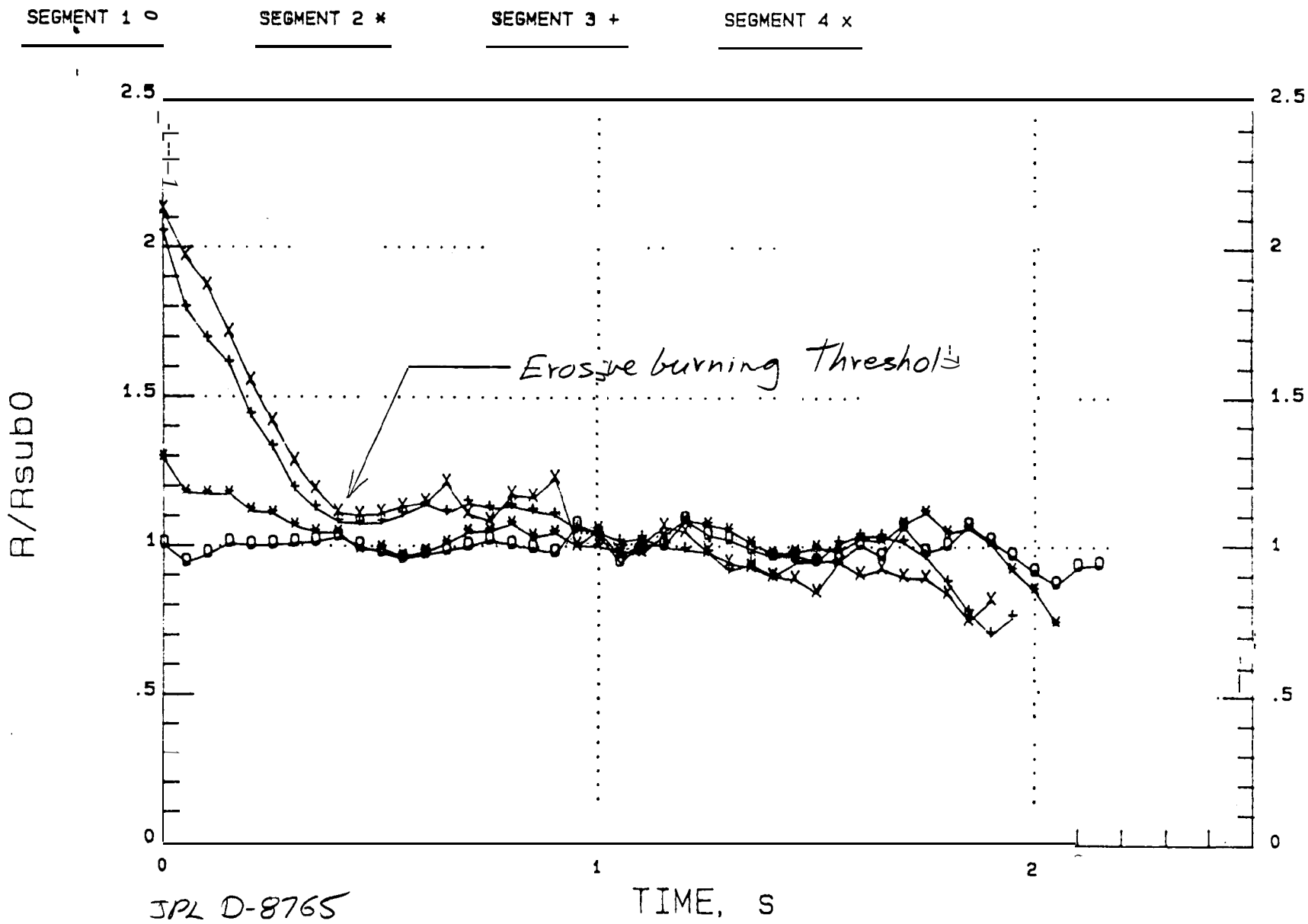

JPL D-8765

LS. 10/6/89

Example of measured burning rate results, normalized by the no-crossflow rates, for a four segment 5x10 motor test

JPL

RADIUS-BASED CROSSFLOW REYNOLDS NO. VERSUS LENGTH-BASED REDUCED SURFACE — TRANSPIRATION REYNOLDS NO. FOR EROSIVE BURNING TRANSITION

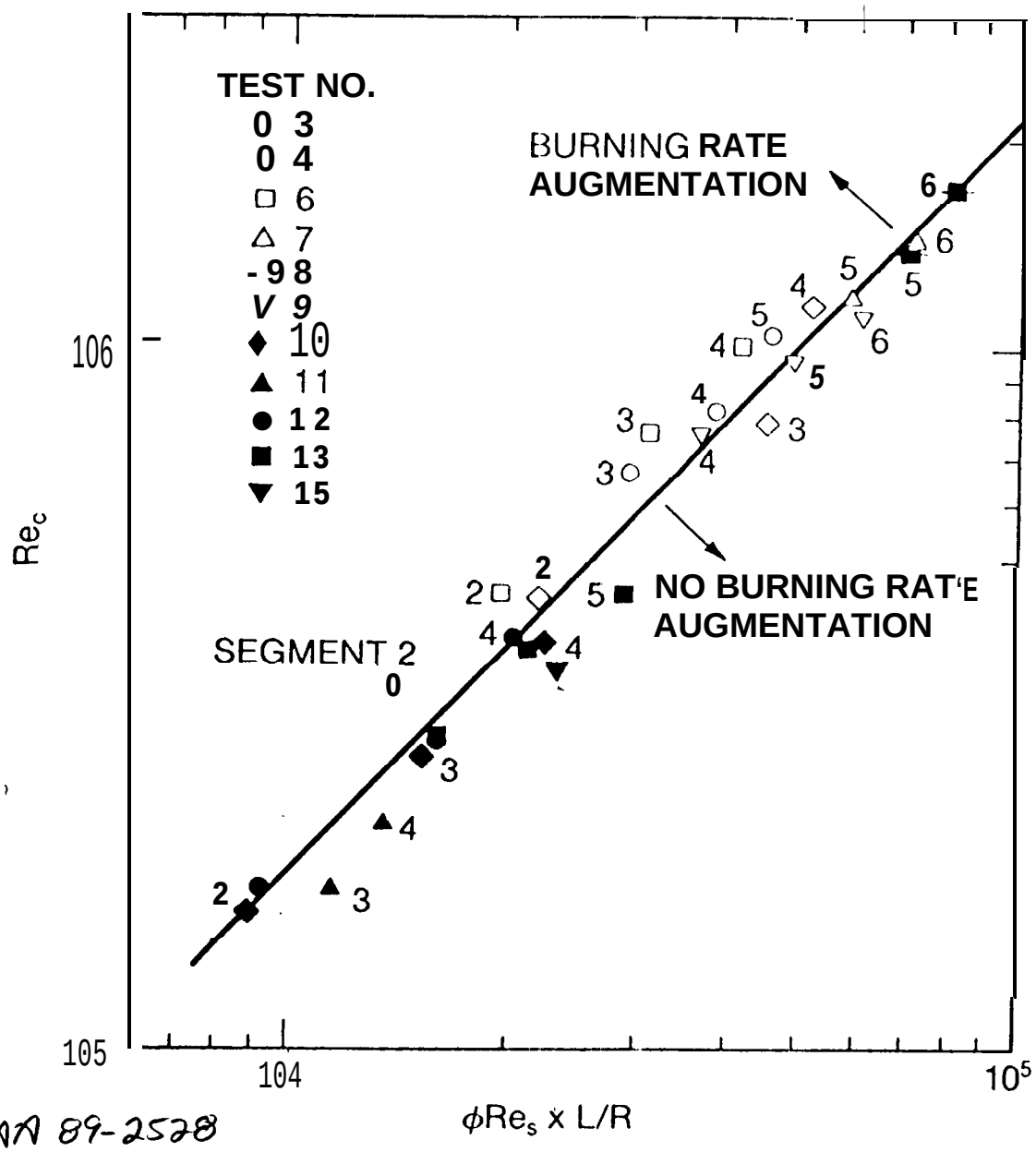

AIAA 89-2528

Correlation of threshold conditions for erosive burning rate augmentation. The critical crossflow mass flux (crossflow Rey. No.) increases with propellant base burning rate (surface-transpiration Rey. No.) and the motor length-to-diameter ratio.

CPIA Publ.
No. 557

Correlating the magnitude of erosive burning rate augmentation by the amount that the Reynolds No. driving parameter exceeds an erosive threshold value. A distinct size scaling effect is apparent for the two different sized rocket motors.

BURN NG RATE AUGMENTATION VS RE NO. -RE NO.,th

PBAN PROPELLANT FORMULATIONS

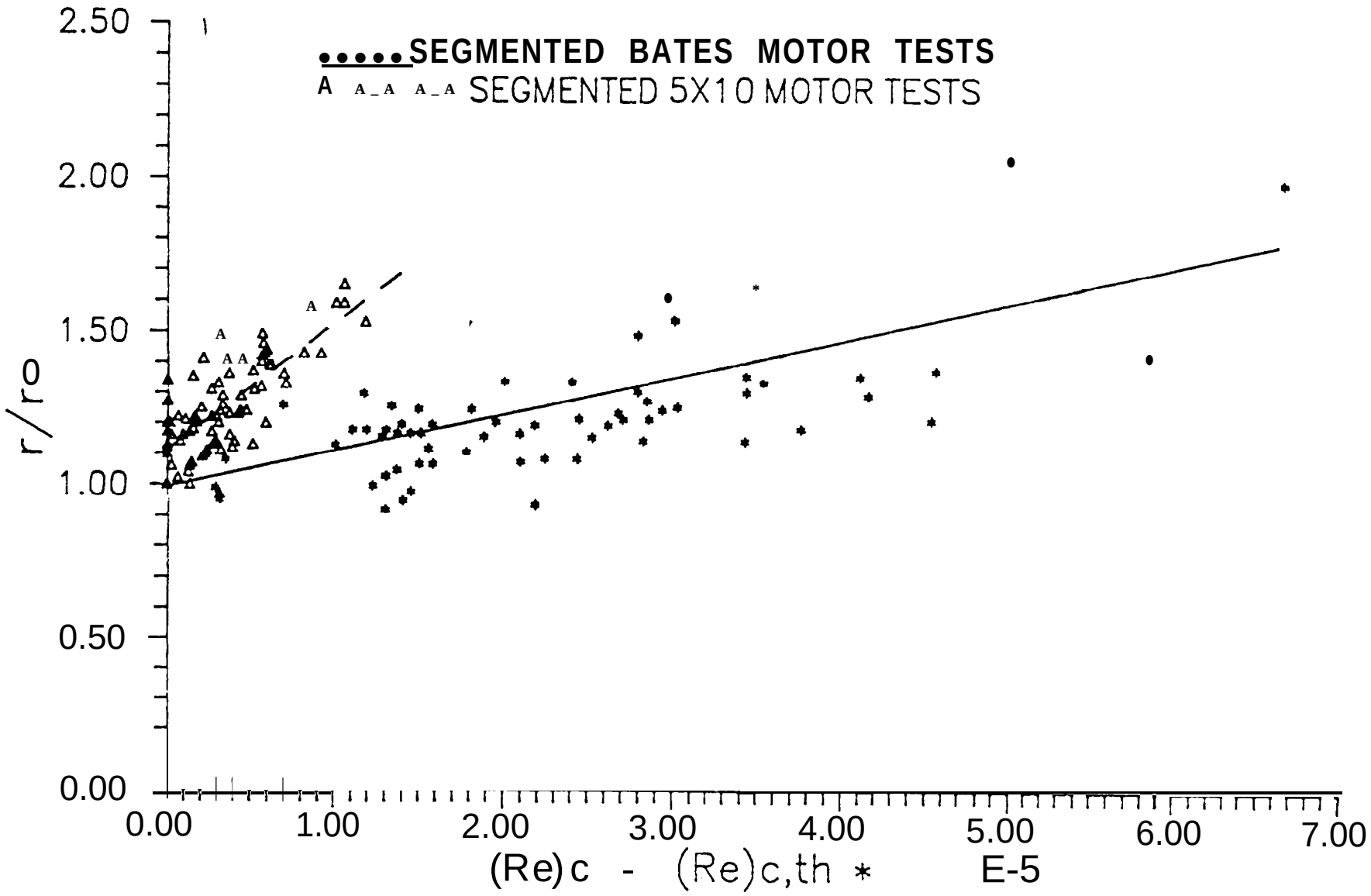

CPIA Publ. No. 557

The size scaling effect was accounted for by adding the motor port radius to the -2.4 power to the independent parameter. The crossflow Reynolds No. was also raised to the 0.8 power, as suggested by correlations for convective heat transfer in pipe flow.

BURNING. RATE AUGMENTATION vs (RE NO.(**0.8)–RE NO.,th(**0.8))/R(**2.4)

PBAN PROPELLANT FORMULATIONS

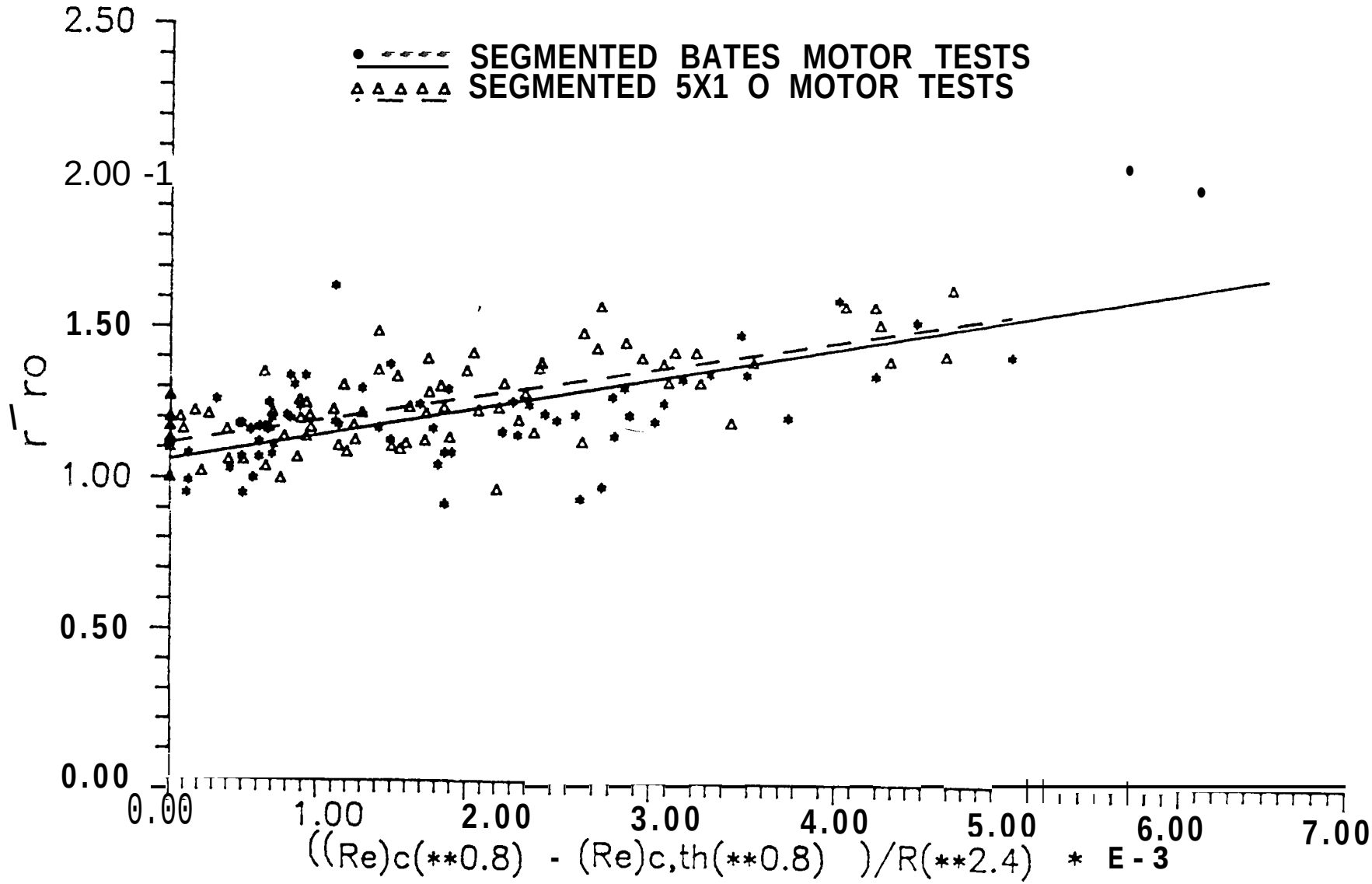

CPIA Publ.
No. 557

Erosive burning rate augmentation with mass flux, G, as the driving parameter. The independent parameter $(G^{0.8} - G_{th}^{0.8}) / R^{0.4}$ provided the required size scaling.

JPL

BURNING RATE AUGMENTATION vs (G(**0.8) – G,th(**0.8))/R(**0.4)

PBAN PROPELLANT FORMULATIONS

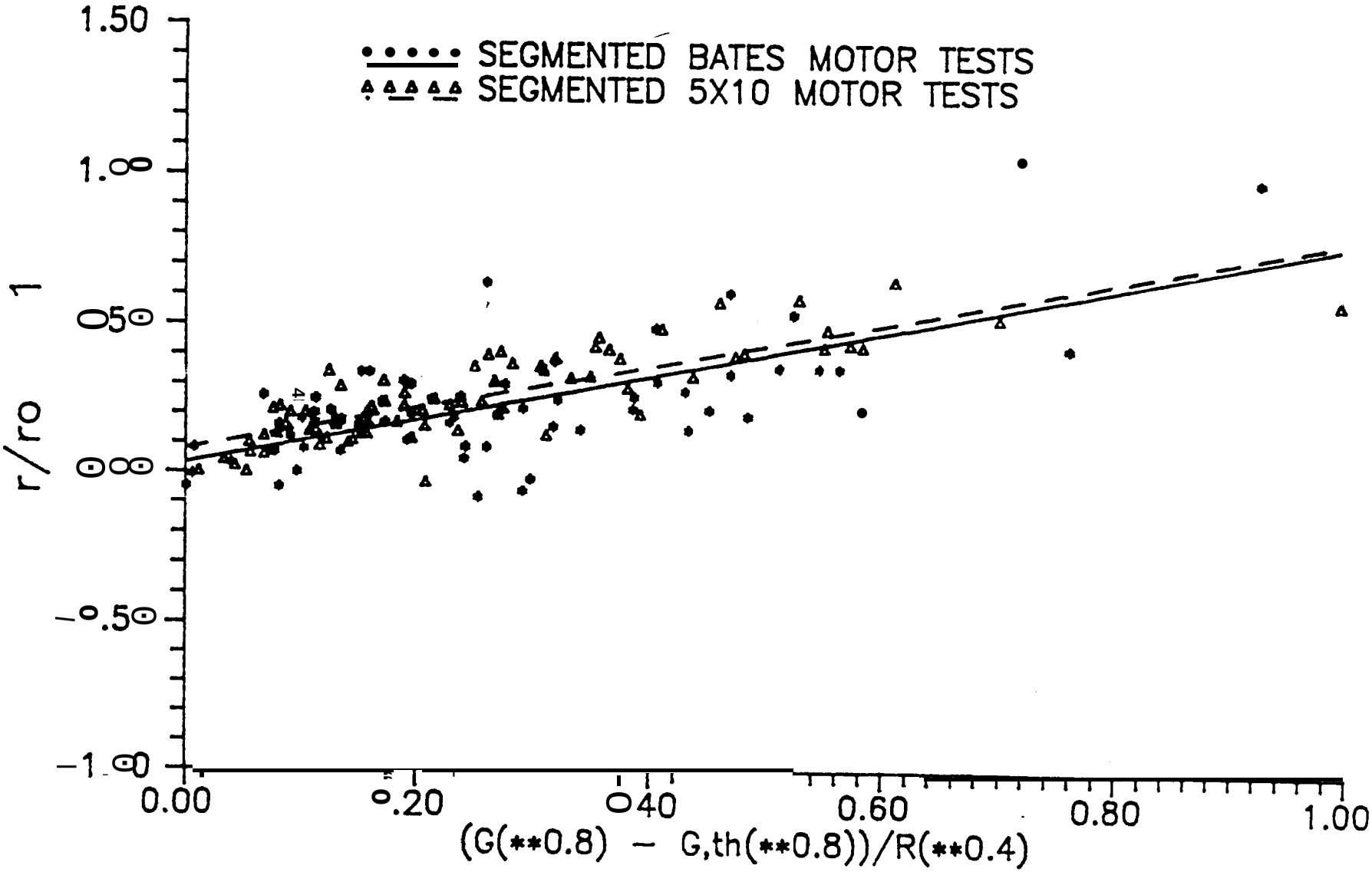

HYBRID ROCKET COMBUSTION INSTABILITY MECHANISMS

AIAA 94-2876

JPL

HYBRID SLAB WINDOW MOTOR

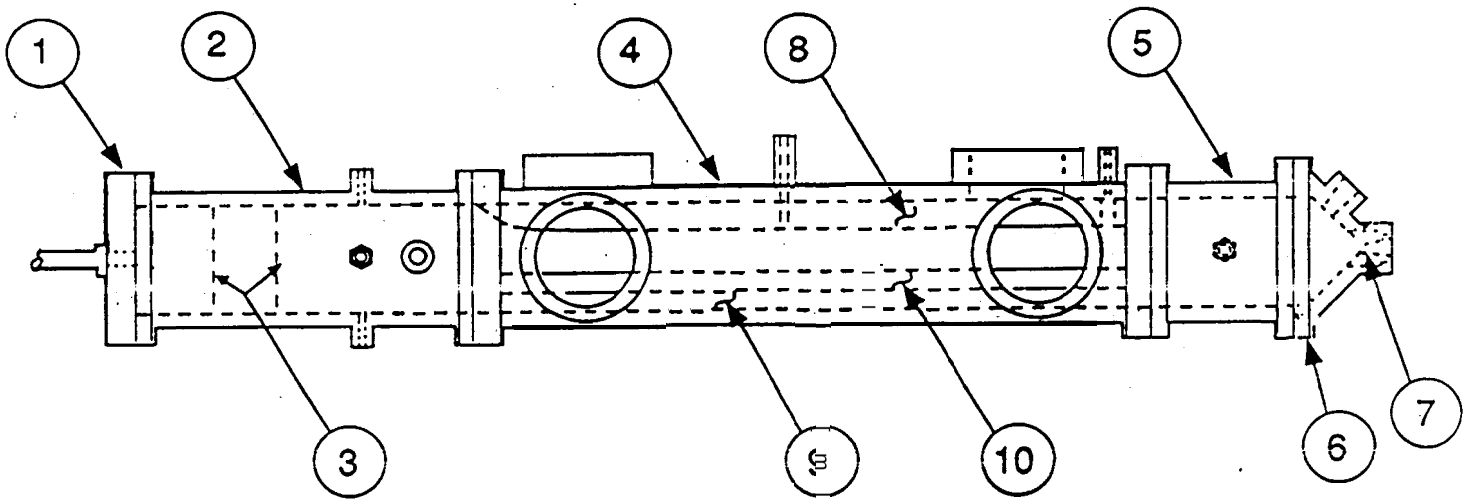

Laboratory hybrid window motor used for fuel decomposition and combustion studies.

AIAA 94-2876

SLAB MOTOR MEASUREMENTS

Parameter	Instrument
CORE GAS TEMPERATURE	MIKRON SERIES M77S 2-COLOR INFRARED THERMOMETER
FUEL SURFACE TEMPERATURE -	MIKRON SERIES M67S INFRARED THERMOMETER (3.86 μm)
TOTAL HEAT FLUX	HYCAL ASYMPTOTIC CALORIMETER
RADIATION HEAT FLUX	HYCAL ASYMPTOTIC RADIOMETER

AIAA 94-2876

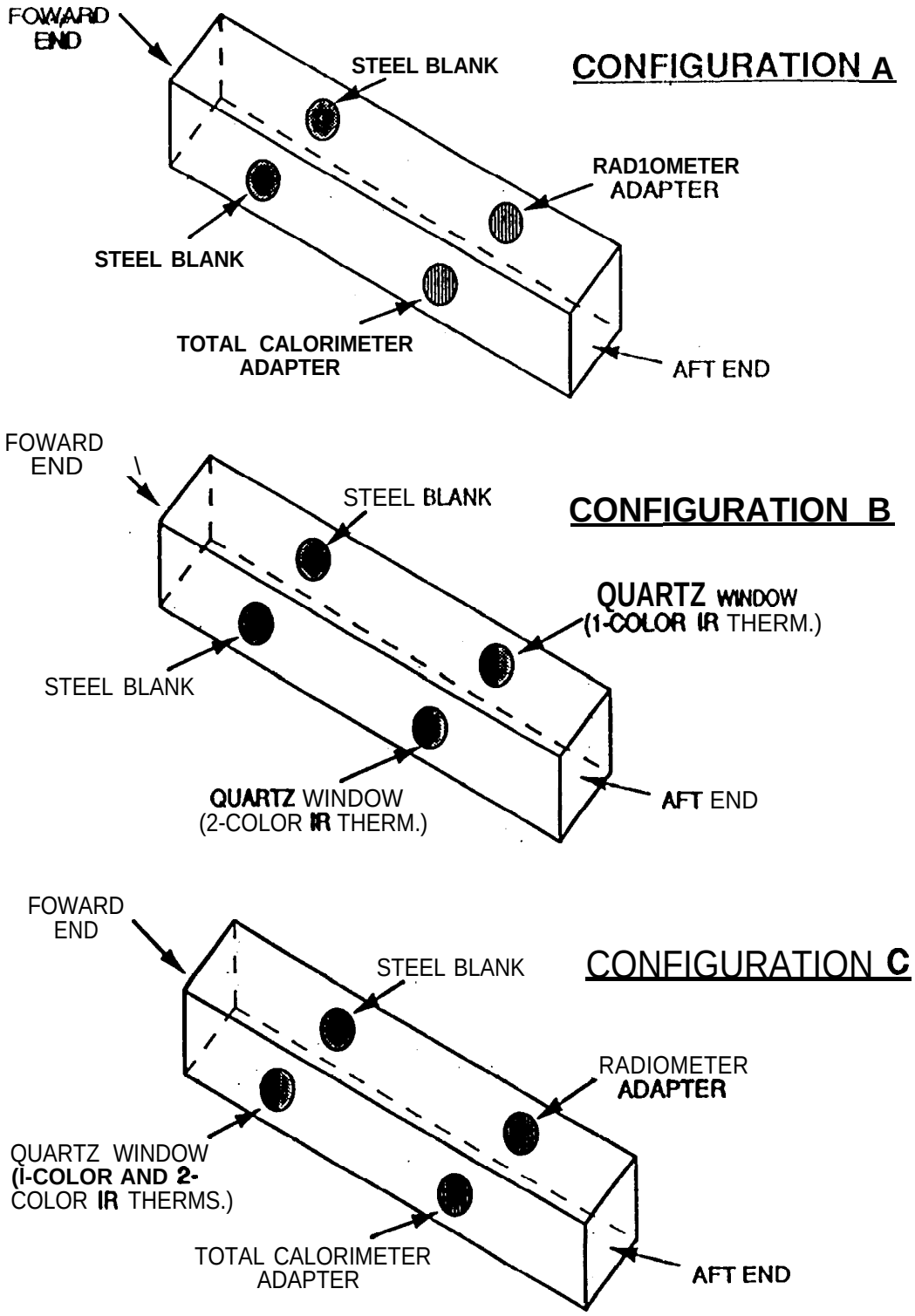

Instrumentation configurations used for the tests.

AIAA 94-2876

COMPARISON OF REGRESSION RATE AND TOTAL HEAT FLUX VARIATIONS vs. TOTAL MASS FLUX

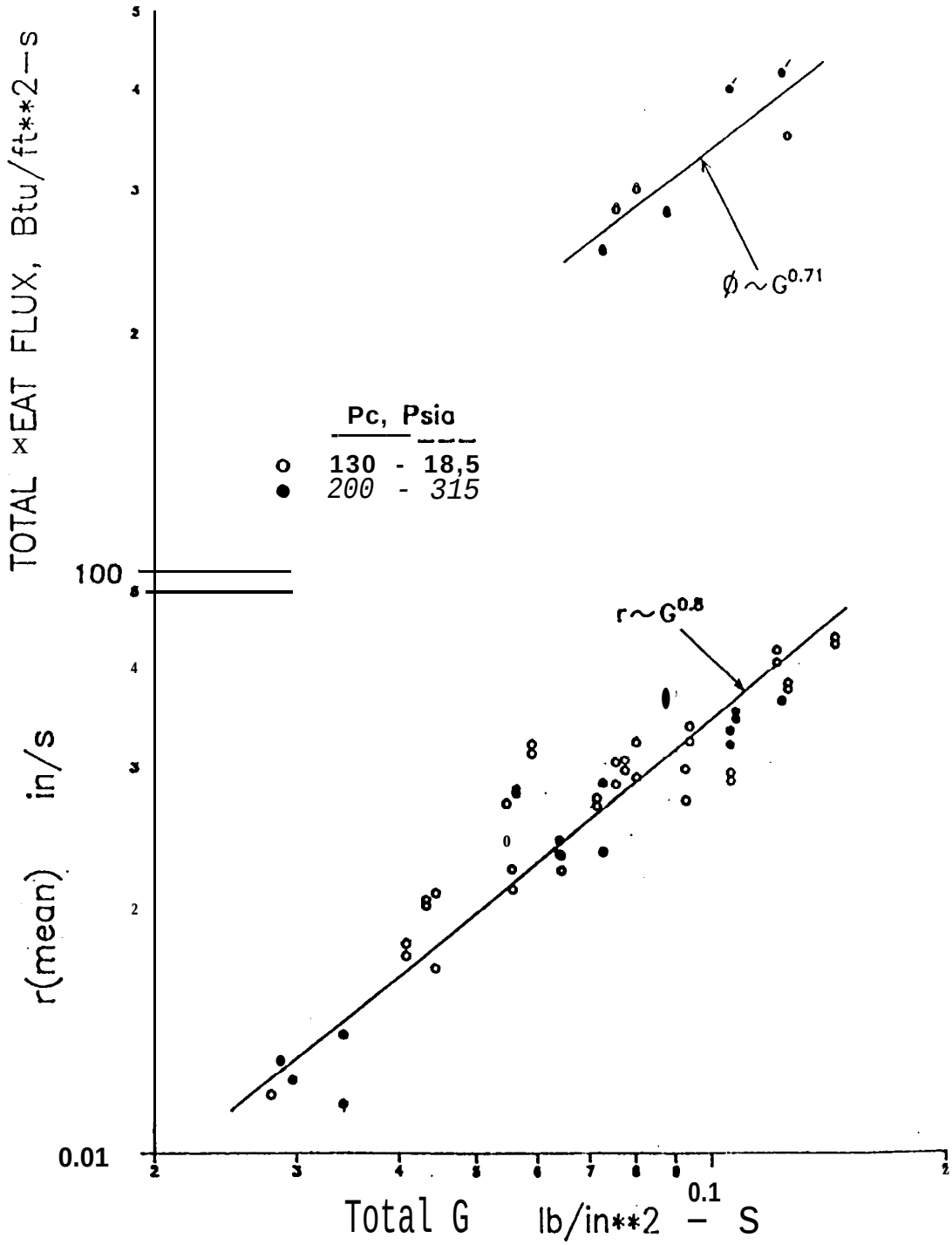

Good agreement in the respective correlations of fuel regression rate and total heat flux through the motor port, indicating a direct dependency of fuel regression on total heat flux to fuel burning surface.

AIAA 94-2876

Simultaneous d.c. shifts in chamber pressure and total heat flux, while rate of oxygen injection remained constant, supporting postulation that the driving mechanism for the sub-acoustic pressure irregularities is some type of flow-combustion turbulence interaction along the fuel surface.

HEAT FLUX & PRESSURE VS TIME

TEST NO. E2091 FUEL: HTPB

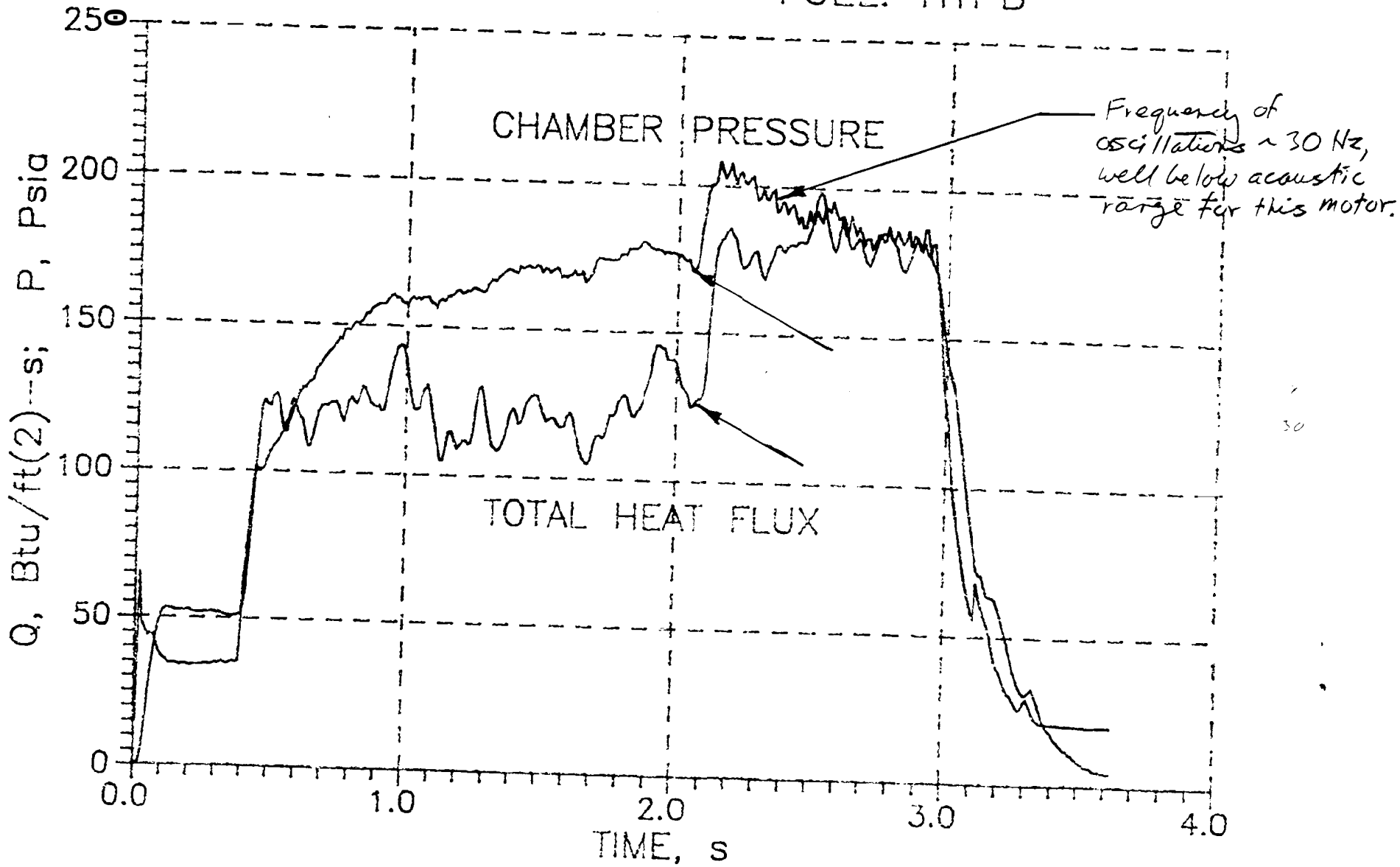

HYBRID

Instability accompanied by d.c. shifts in gas (positive) and fuel surface (negative) temperatures

AIAA 94-2876

TEMPERATURE vs TIME

TEST NO. E2091 FUEL: HTPB

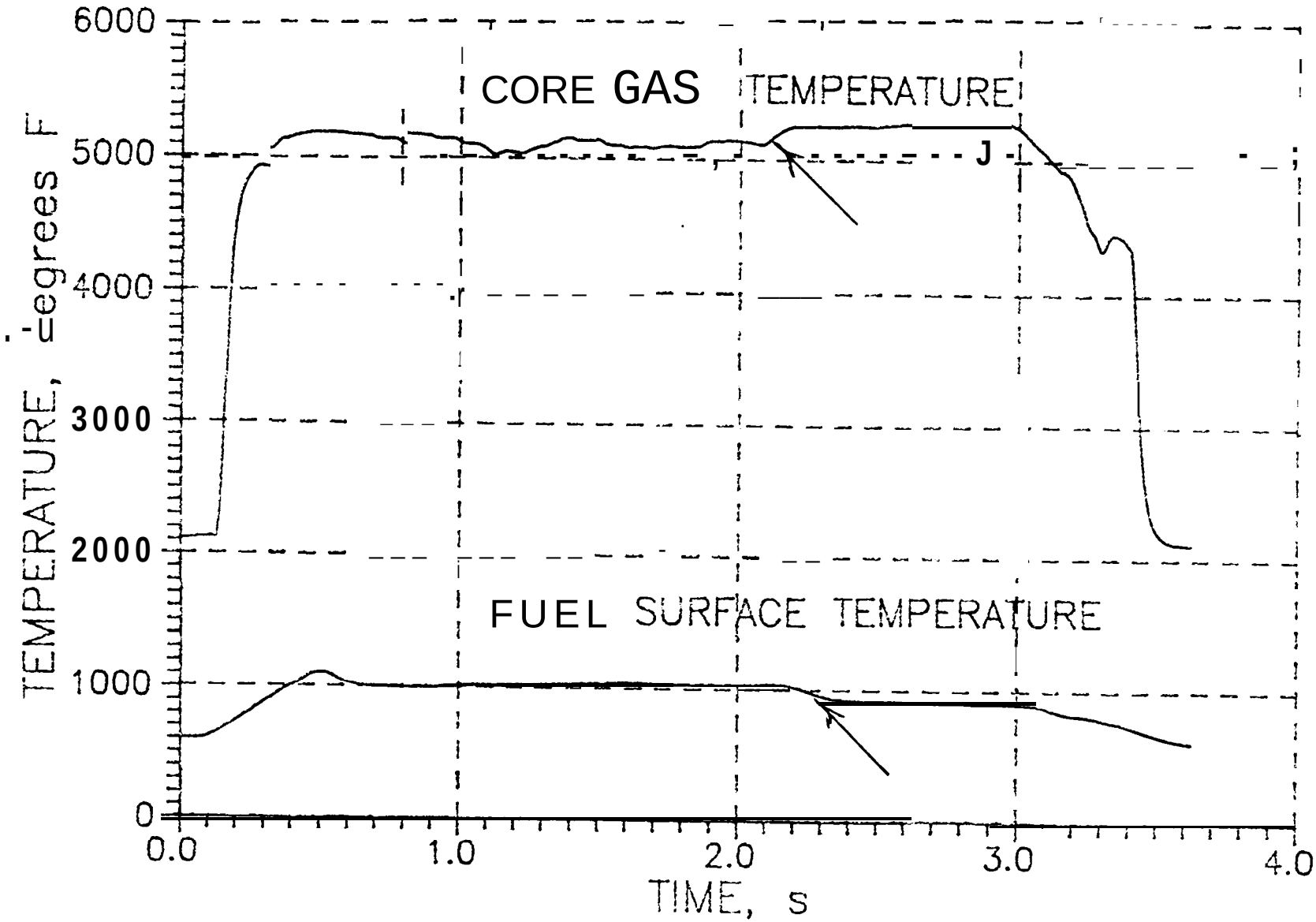

HYBRID
05/05/94

MINIATURIZED COMPONENTS FOR FUTURE SPACECRAFT PROPULSION SYSTEMS

AIAA 94-3374

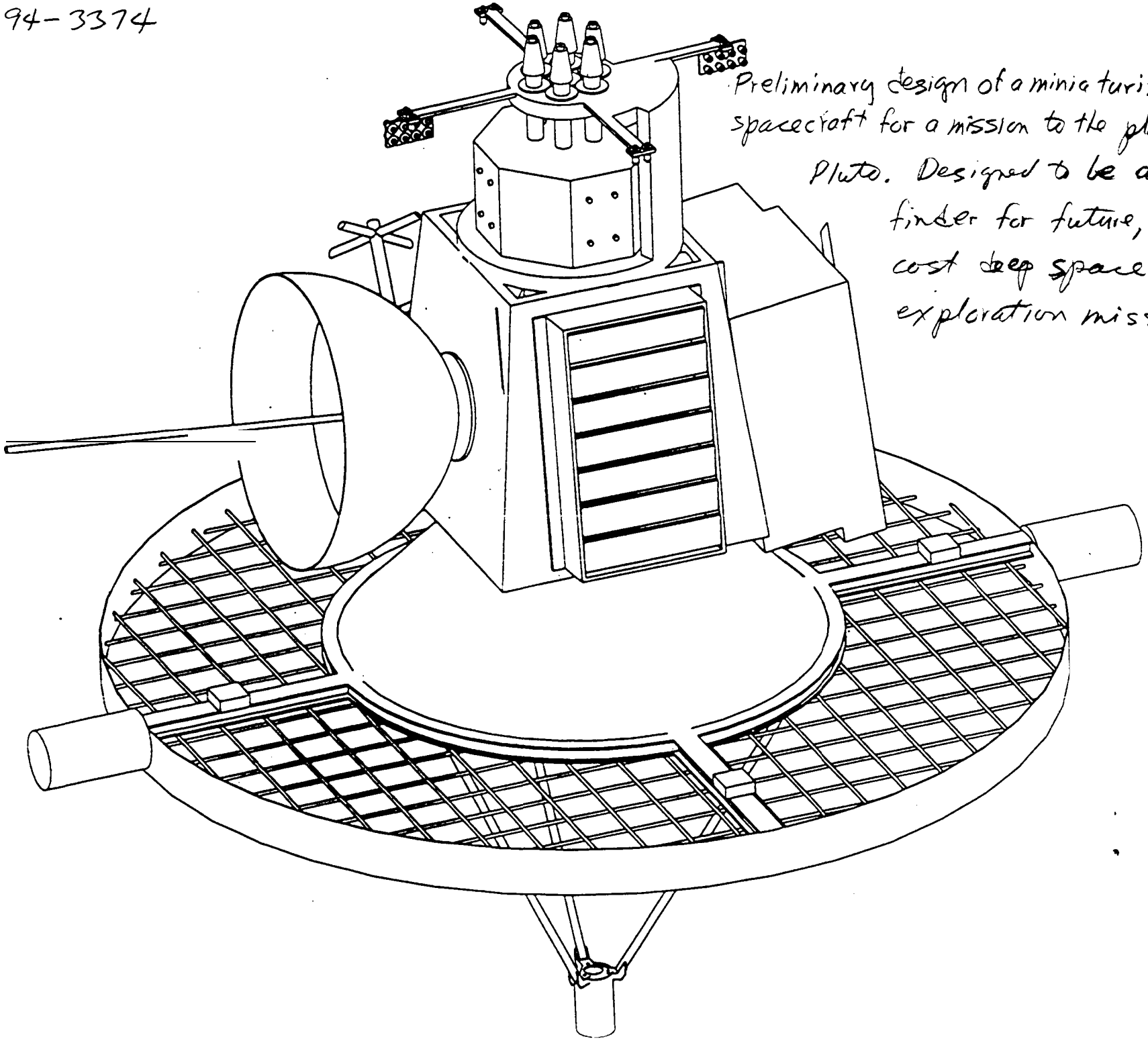

Preliminary design of a miniaturized spacecraft for a mission to the planet Pluto. Designed to be a path-finder for future, lower cost deep space exploration missions.

AIAA 94-3374

JPL PLUTO FAST FLYBY - SPACECRAFT PROPULSION

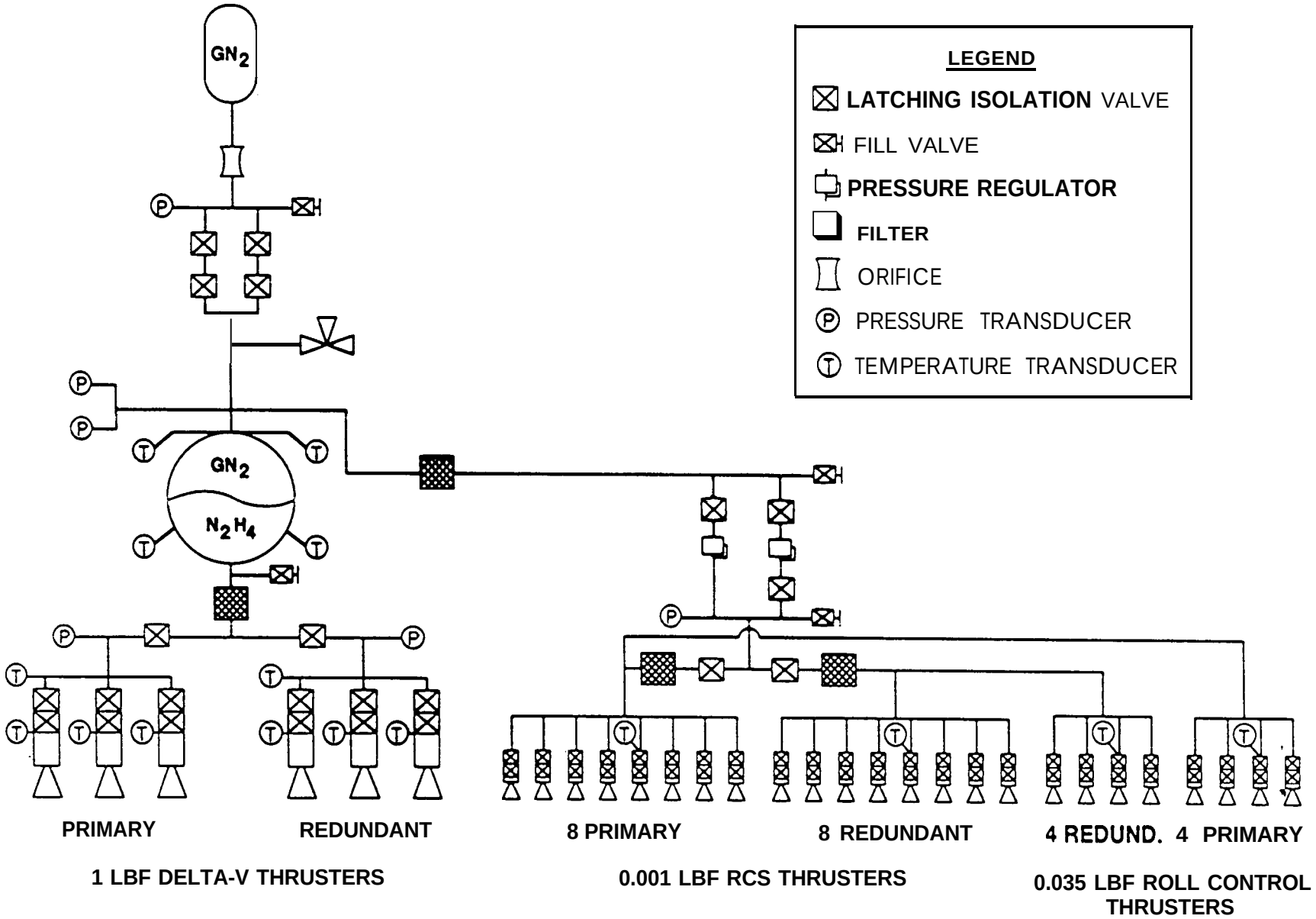

Schematic of candidate monopropellant hydrazine (course correction) and cold-gas (attitude and roll control) propulsion system.

AIAA 95-2810

ATI BREADBOARD TEST SYSTEM

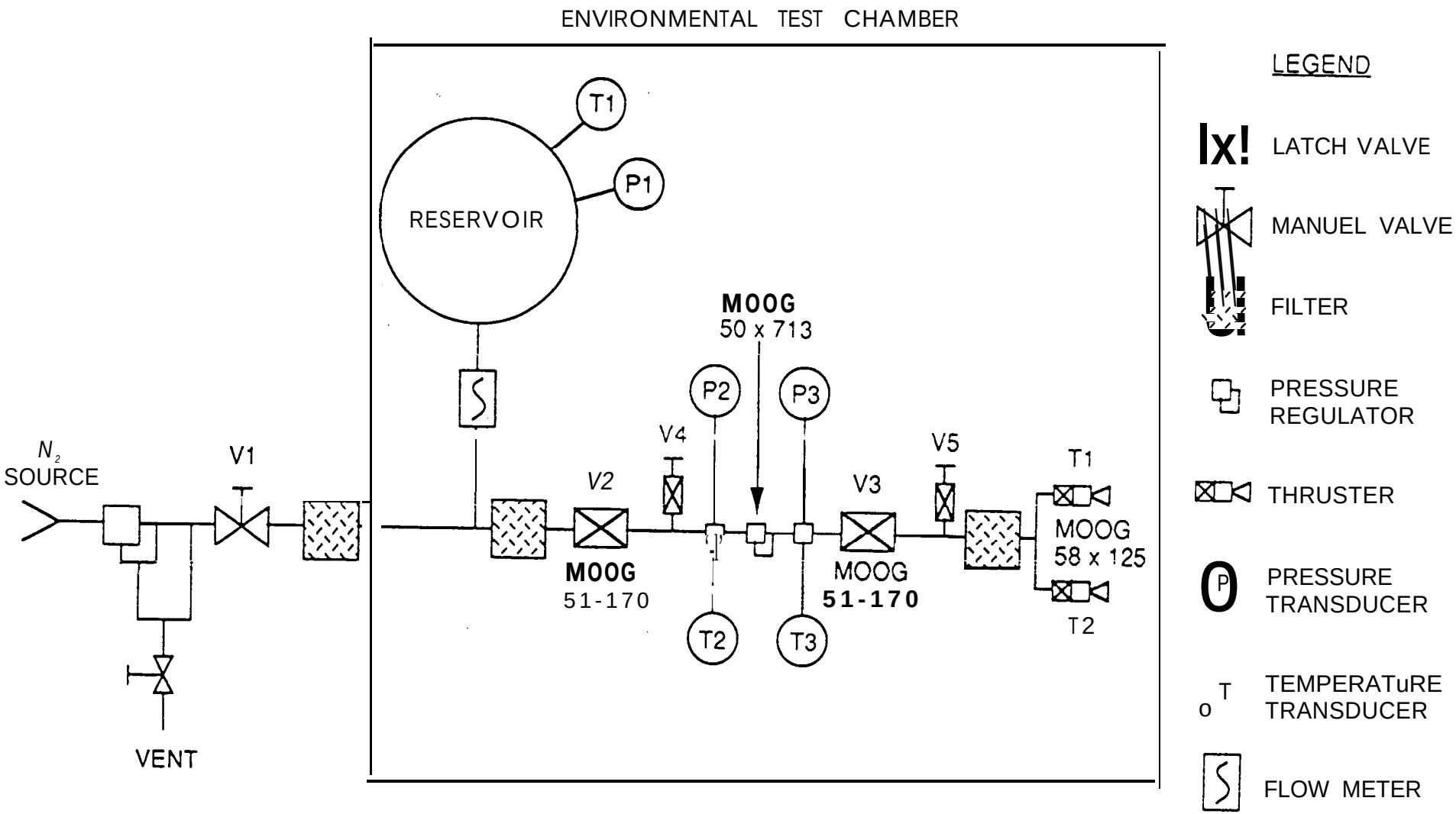

Test system was used for testing prototype cold-gas propulsion components at simulated space flight temperature conditions.

AIAA 95-2810
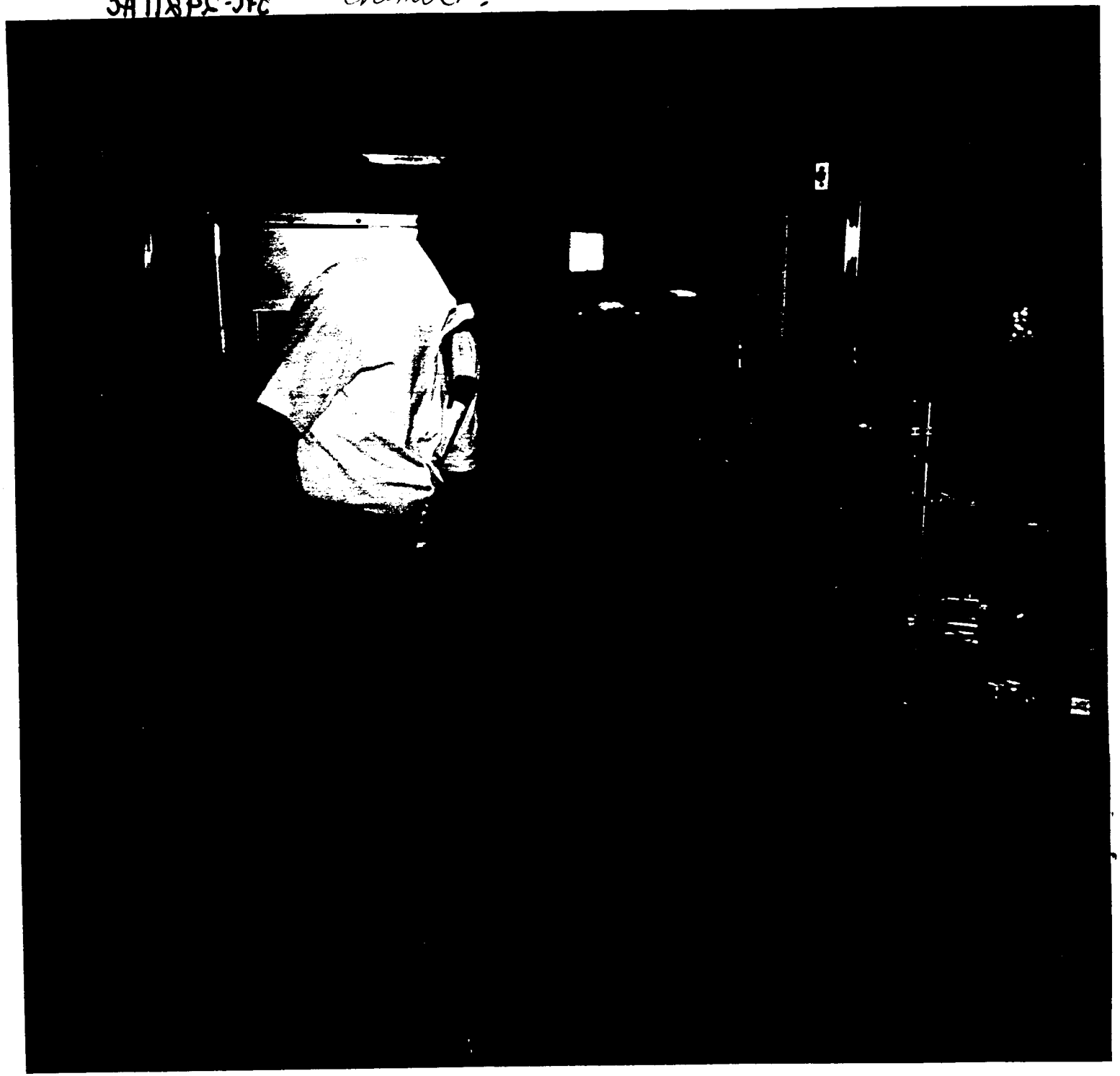
Breadboard test system in temperature conditioning chamber.